

## Thermodynamic Properties of Methanol in the Critical and Supercritical Regions

I. M. Abdulagatov,<sup>1,2</sup> N. G. Polikhronidi,<sup>2</sup> A. Abdurashidova,<sup>1</sup>  
S. B. Kiselev,<sup>3,4</sup> and J. F. Ely<sup>3</sup>

*Received June 2, 2005*

---

The isochoric heat capacity of pure methanol in the temperature range from 482 to 533 K, at near-critical densities between 274.87 and 331.59 kg·m<sup>-3</sup>, has been measured by using a high-temperature and high-pressure nearly constant volume adiabatic calorimeter. The measurements were performed in the single- and two-phase regions including along the coexistence curve. Uncertainties of the isochoric heat capacity measurements are estimated to be within 2%. The single- and two-phase isochoric heat capacities, temperatures, and densities at saturation were extracted from experimental data for each measured isochore. The critical temperature ( $T_c = 512.78 \pm 0.02$  K) and the critical density ( $\rho_c = 277.49 \pm 2$  kg·m<sup>-3</sup>) for pure methanol were derived from the isochoric heat-capacity measurements by using the well-established method of quasi-static thermograms. The results of the  $C_VVT$  measurements together with recent new experimental  $PVT$  data for pure methanol were used to develop a thermodynamically self-consistent Helmholtz free-energy parametric crossover model, CREOS97-04. The accuracy of the crossover model was confirmed by a comprehensive comparison with available experimental data for pure methanol and values calculated with various multiparameter equations of state and correlations. In the critical and supercritical regions at  $0.98T_c \leq T \leq 1.5T_c$  and in the density range  $0.35\rho_c \leq \rho \leq 1.65\rho_c$ , CREOS97-04 represents all available experimental thermodynamic data for pure methanol to within their experimental uncertainties.

---

**KEY WORDS:** coexistence curve; critical region; crossover equation of state; methanol; isochoric heat capacity; thermodynamic properties.

---

<sup>1</sup> Institute for Geothermal Problems of the Dagestan Scientific Center of the Russian Academy of Sciences, Shamilya Street 39-A, 367003 Makhachkala, Dagestan, Russia.

<sup>2</sup> Institute of Physics of the Dagestan Scientific Center of the Russian Academy of Sciences, Yaragskogo Street 94, 367005 Makhachkala, Dagestan, Russia.

<sup>3</sup> Chemical Engineering Department, Colorado School of Mines, Golden, Colorado 80401-1887, U.S.A.

<sup>4</sup> To whom correspondence should be addressed. E-mail: skiselev@mines.edu

## 1. INTRODUCTION

Fluids of species that exhibit hydrogen bonding behave differently from systems of molecules that interact only through dispersion forces, especially in the critical and supercritical regions. In these fluids, strong attractive interactions between molecules result in the formation of molecular clusters that have considerable effect on the thermodynamic and structural properties of the species. Therefore, the anomalous structural and thermodynamic properties of highly associated fluids like *n*-alkanols are strongly affected by the hydrogen bonding. Due to their high polarity and strong self-association, *n*-alkanols, and in particular methanol, are complex fluids and extremely challenging materials for both experimental and theoretical study. Experiments that measure thermodynamic properties over a wide temperature range of light alkanols are often hindered by chemical reactions, including decomposition. A number of previous studies have explored the effects of reactions on the properties of methanol [1–7]. It has been reported that a serious complication exists when  $T > 405$  K, since methanol begins to decompose at this temperature [1, 2, 4, 7]. In mixtures where methanol is one of the components, the thermodynamic properties may also exhibit anomalies due to H-bonded molecular associations. For example, methanol molecules strongly affect water structure and, as a consequence, various physical properties in water + methanol mixtures exhibit strong anomalies [8–10].

The design of engineering systems utilizing methanol requires an accurate knowledge of thermodynamic properties. It is well known that the addition of a polar co-solvent (methanol, for example) to supercritical H<sub>2</sub>O or CO<sub>2</sub> often leads to an enhancement in the solubility of a solute and can improve the selectivity of a supercritical solvent (effective polar modifiers) [11–18]. Thus, Methanol is often used as an effective modifier for H<sub>2</sub>O and CO<sub>2</sub> in supercritical fluid extraction and in supercritical chromatography. However, because of the complexity of methanol, there are neither representative experimental data nor predictive thermodynamic models available that will offer sufficient insight for optimum process design. Existing semi-empirical and statistical-mechanics-based thermodynamic models [19–27] have not yet been developed to a degree that they can be used for an accurate prediction of the thermodynamic properties of methanol in the critical and supercritical regions. Therefore, development of a thermodynamically self-consistent theoretically based model for prediction of thermodynamic properties of methanol close to and far away from the critical point is an important goal.

The major objective of this paper is to provide heat capacity  $C_v$  and the saturation properties ( $T_s$ ,  $P_s$ ,  $\rho_s$ ) for methanol in the critical region

and to develop on this basis a thermodynamically self-consistent fundamental equation for methanol at near-critical and supercritical conditions.

## 2. PREVIOUS EXPERIMENTAL DATA FOR METHANOL IN THE CRITICAL REGION

Due to the thermal instability of methanol, thermodynamic data obtained by different authors display a larger scatter than the reported uncertainties in the individual experimental data sets. This makes it extremely difficult to select primary thermodynamically consistent data sets for developing an accurate equation of state. At the present time, there are some compilations of the thermodynamic properties of methanol, namely, those reported by IUPAC [22], Eubank [28], Aliev et al. [29], and Zubarev et al. [30]. Experimental thermodynamic data for pure methanol prior to 1993 were reviewed and compiled extensively under the auspices of IUPAC [22] and have been reported in the International Thermodynamic Tables of the Fluid State-12 [22]. Since then, new experimental data for methanol have appeared in the literature, which we have reviewed in a previous publication [29]. Therefore, we review here only the primary data sets used for developing an equation of state in the critical region and some selected secondary data sets used for the testing of the equation. A brief analysis of the different thermodynamic property data sets and the correlations in the critical and supercritical regions of methanol is given below.

### 2.1. PVT Properties in the Single-Phase Region

*PVT* measurements of pure methanol in the critical region are very limited. Recently Bazaev et al. [7] reported *PVT* measurements of pure methanol at near-critical and supercritical conditions. These measurements were obtained with a constant-volume piezometer immersed in a precision thermostat in the temperature range from 423 to 653 K, at densities from 113 to 370 kg·m<sup>-3</sup>, and at pressures from 1.4 to 40 MPa. The uncertainty of the temperature, density, and pressure measurements were 15 mK, 0.2%, and 0.05%, respectively. The purity of the methanol sample was 99.93 mol%. At temperatures starting around 180–200 °C thermal decomposition of methanol was observed.

Straty et al. [2] have reported high-temperature and high-pressure *PVT* measurements for compressed gas and liquid methanol in the temperature range from 373 to 573 K and for densities between 64 and 704 kg·m<sup>-3</sup>. The uncertainty in the density measurements was 0.2%. The pressure was measured with an uncertainty of 0.05%. The methanol samples were 99.90% pure. They found the rate of change of pressure due

to degradation of the methanol sample to be proportional to the density and temperature. Pressure-corrected data were compared with values reported by Zubarev and Bagdonas [31] and Machado and Streett [25] in the region of overlap. Excellent agreement was found at low temperatures and high densities with data reported by Machado and Street [25]. Agreement between Straty et al. [2] and the data reported by Zubarev and Bagdonas [31] is about 0.2%, which, except at low densities and in the critical region, is very close to their experimental uncertainties. However, the differences between these data and the data reported by Finkelstein and Stiel [32] are considerably larger (about 2.5%). Zubarev and Bagdonas [31] have performed *PVT* measurements in the temperature range from 322 to 573 K and at pressures between 0.4 and 20 MPa with a constant-volume piezometer. The uncertainty of the reported data is 0.2–0.3%, except in the critical region. The scatter of the derived experimental data is within 0.1–0.15%. The organic content of the methanol sample was 0.05%. After the measurements were completed, the water content in the sample was 0.16–0.2%. Decomposition of the methanol molecules in the supercritical region up to 513 K was not observed. The values of the compressibility factor *Z* derived from these *PVT* data agree with data reported by Ramsey and Young [33] at 503 K within  $\pm 3\%$ . Ta'ani [3] has reported *PVT* data of methanol at temperatures between 298 and 623 K and at pressures up to 800 MPa, and have also observed a decomposition effect on the measured values of *PVT*.

## 2.2. Vapor Pressures

Ambrose and Walton [34] have proposed a vapor-pressure equation for pure methanol up to the critical temperature. To represent available vapor-pressure data of methanol, they used an equation proposed by Wagner [35] with system-dependent constants. An IUPAC formulation, developed by de Reuck and Craven [22], also incorporates a Wagner type four-constant vapor-pressure equation. Recently, Kozlov [27] reported a new polynomial type vapor-pressure equation for pure methanol in the temperature range from the triple to the critical point. The uncertainty of the correlation is 0.27%. Goodwin [23] has proposed a nonanalytical type vapor-pressure equation for pure methanol (root-mean-square error,  $\text{RMS} = 0.34\%$ ) in the range from the triple to the critical point. Zubarev et al. [30] have adopted a polynomial-type equation to represent their vapor-pressure data. All available experimental vapor-pressure data of pure methanol together with values calculated from various correlations are shown in Fig. 1. Comparisons of vapor pressures calculated from the equation developed by Ambrose and Walton [34] with values calculated

from the correlations reported by other authors are shown in Fig. 2. The differences between various correlations in the critical region (from 490 to 512.6 K) are  $\pm 0.5\%$ .

Very few experimental vapor-pressure data in the critical region are available in the literature for pure methanol (see Fig. 1). Recently Bazaev et al. [7] used isothermal ( $P-\rho$ ) and isochoric ( $P-T$ ) break point techniques to extract vapor-pressure data from precise  $PVT$  measurements in the temperature range from 423.15 to 503.15 K. These data agree with values calculated from correlations [22, 23, 27, 30, 34] and reported experimental data [25, 31, 36–40] to within 0.2–0.4%. Lydersen and Tsochev [37] have reported vapor pressures for pure methanol in the temperature range from 494.8 to 511.75 K. These data are about 0.1% higher than the data reported by Zubarev and Bagdonas [31] and by de Loos et al. [39], while the data obtained by Kay and Donham [41] and Ambrose et al. [40] are higher by 0.3% and 0.2%, respectively. Agreement to within 0.3% is observed between the data of Lydersen and Tsochev [37] and the data of Bazaev et al. [7]. de Loos et al. [39] reported vapor-liquid equilibrium data for pure methanol obtained by using a high-pressure capillary glass-tube apparatus in the temperature range from 422 to 512.5 K.

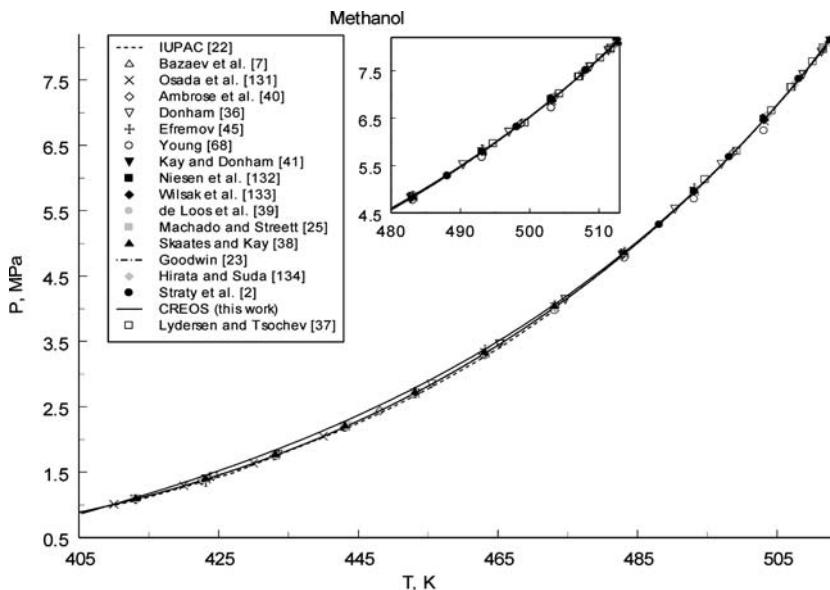


**Fig. 1.** Available experimental vapor pressure data of methanol reported by different authors [2, 7, 25, 36–41, 45, 68, 131–134] together with values calculated from CREOS97-04 and various correlation equations [22, 23, 122].

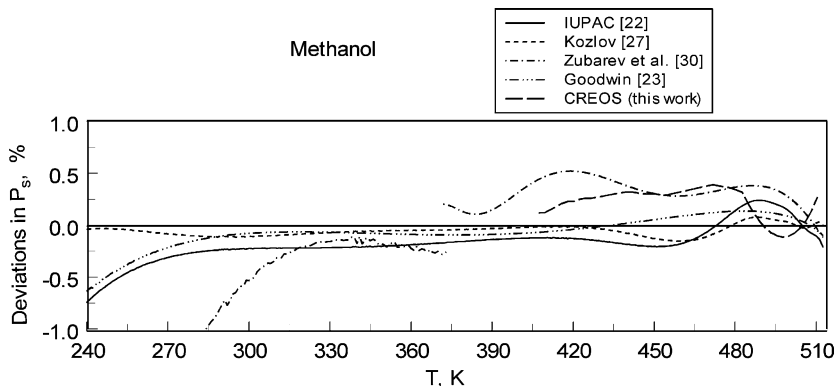


Fig. 2. Comparison of vapor pressures of methanol calculated with correlation by Ambrose and Walton [34] with values calculated with CREOS97-04 and various correlations developed by other authors [22, 23, 27, 30].

At temperatures above 455 K, the vapor-pressure data of de Loos et al. [39] agree to within 0.05 MPa with the recommended IUPAC values [22]. Zubarev and Bagdonas [31] have reported 32 values of vapor-pressure data in the temperature range between 373 and 513 K.

Donham [36] has reported vapor–liquid–equilibrium data ( $T_S$ ,  $P_S$ ,  $\rho_S''$ ,  $\rho_S'$ ) for pure methanol and methanol + hydrocarbon mixtures. The uncertainties of the data are 0.05 K, 0.35 MPa, and 1.0% for the temperature, pressure, and density, respectively. The measurements were made up to the critical temperature by using a thick-walled glass tube which was surrounded by a constant-temperature bath. Skaates and Kay [38] have reported vapor-pressure data for methanol in the temperature range from 403 to  $T_c = 512.64$  K. These data agree with values reported by Bazaev et al. [7] to within 0.13%. Ambrose et al. [40] extended earlier vapor-pressure measurements for methanol up to 462.9 K. The measurements were made by a dynamic method [40]. A Chebyshev polynomial equation was fitted to the results of the measurements. Overall, the available experimental vapor-pressure-data sets contain only 30 experimental data in the temperature range from 482 K to  $T_c$ .

### 2.3. Saturated Densities

Limited experimental saturated liquid and vapor density data sets are available for pure methanol in the critical region. Suleimanov [42] reported saturated densities for pure methanol (maximum water content of less than 0.04% and an organic content less than 0.02%) in the critical

region using the discontinuity of the ischoric heat-capacity measurements as the intersection of the phase-transition points. Fifteen values of the saturated liquid and vapor densities have been reported by Suleimanov [42] in the temperature range from 483.15 K to the critical temperature. The measured saturated liquid,  $\rho'_s$ , and vapor,  $\rho''_s$ , densities were fitted to the expressions,

$$\rho'_s/\rho_c = 1 + 2.58t^{0.366}, \quad \rho''_s/\rho_c = 1 - 1.978t^{0.327}, \quad (1)$$

where  $t = 1 - T/T_c$ ,  $\rho_c = 267.38 \text{ kg} \cdot \text{m}^{-3}$ , and  $T_c = 512.70 \pm 0.2 \text{ K}$ .

Polikhronidi et al. [5] also used isochoric heat-capacity experiments together with a quasi-static-thermogram technique to obtain saturated densities for pure methanol in the critical region. They reported 22 values of the saturated boundary properties ( $T_S, \rho''_S, \rho'_S$ ) for pure methanol including in the critical region. The uncertainty of the phase-transition temperature and density measurements were, respectively, 0.02 K and 0.15%. Six values of the saturated density and saturated temperature were obtained from these  $C_V VT$  measurements by Abdulagatov et al. [4]. Bazaev et al. [7] used isothermal ( $P-\rho$ ) and isochoric ( $P-T$ ) break-point techniques to extract saturated densities for methanol in the temperature range from 423.15 to 503.15 K. These data show good agreement (average absolute deviations, AAD, within 0.06–0.5%) with the data reported in the literature and those calculated from various correlations.

Cibulka [44] has critically evaluated all published experimental saturated-liquid densities for pure methanol and reported a non-scaling type equation and recommended values for the saturated-liquid densities of pure methanol. The temperature range for the experimental saturated density data is from 175.4 to 508.51 K. The relative RMS of the correlation was 0.18%, or  $1.03 \text{ kg} \cdot \text{m}^{-3}$ . Unfortunately, this correlation does not include the critical region between 508.51 K and  $T_c$ . All of the available experimental saturated-liquid and -vapor densities of methanol together with values calculated from various correlation equations are shown in Fig. 3. Comparisons of the saturated liquid densities calculated from the equation proposed by Cibulka [44] with values calculated from the various correlations reported by other authors are shown in Fig. 4. The differences between various correlations in the critical region (from 490 to 512.6 K) are up to  $\pm 2\%$ . The same difference (about 2%) is found between the critical densities reported by various authors (see Fig. 5 and Table I). Overall, we found 43 experimental data points in the literature in the temperature range from 505 K to  $T_c$ . The data of Ramsey and Young [33] and Efremov [45] are systematically off by almost 8 to 10% in this region.

**Table I.** Reported Values of the Critical Properties of Methanol

$T_c$ (K)	$P_c$ (MPa)	$\rho_c$ ( $\text{kg} \cdot \text{m}^{-3}$ )	References
505.9 ± 0.2	7.382 ± 0.12	–	Hannay [55]
506.20	7.0650	–	Nedejdine [56]
513.20	7.9590	271.5	Ramsay and Young [33]
536.20	–	–	de Heen [57]
513.40	–	–	Schmidt [58]
515.20	–	–	Schmidt [59]
513.4 ± 0.2	–	275.0	Centnerszwer [60]
513.70	–	–	Crismer [61]
513.20	7.9540	272.2	Young [68]
513.20	9.7010	358.7	Salwedel [62]
513.80	–	–	Fischer and Reichel [69]
505.20	–	–	Golik et al. [63]
512.6 ± 0.05	8.097 ± 0.003	272.0 ± 6	Kay and Donham [41]
513.20	–	–	Nozdrev [54]
513.20	–	271.0	Krichevskii et al. [70]
513.20	7.9570	–	McCracken et al. [119]
513.90	–	–	Mocharnyuk [64]
512.68 ± 0.22	8.0940	–	Skaates and Kay [38]
513 ± 1.0	7.9743	272.0	Efremov [45]
512.7 ± 0.3	8.104 ± 0.04	275.0 ± 8	Zubarev and Bagdonas [31]
514.70	–	–	Marshall and Jones [71]
512.32 ± 0.1	8.000 ± 0.002	–	Kay and Khera [65]
512.60	8.1000	–	Francesconi et al. [66]
512.43 ± 0.1	8.072 ± 0.005	–	Brunner et al. [67]
512.5 ± 0.2	8.060 ± 0.02	–	de Loos et al. [39]
512.50	8.0600	–	Lydersen and Tsochev [37]
512.5 ± 0.2	8.084 ± 0.02	273.0 ± 2	Gude and Teja [80]
512.78	7.9842	–	Eubank [28]
513.15	–	–	Costello and Bowden [120]
512.64	–	272.0	Ambrose and Townsend [121]
513.00	7.9743	272.0	Loktev [122]
512.60	–	–	Yerlett and Wormald [1]
512.64	8.0920	272.0	Ambrose and Walton [34]
512.58	8.0970	271.8	Donham [36]
–	8.1038	276.0	Harrison and Gammon [123]
512.60	8.1035	276.0	Kozlov [27]
512.60	7.8200	–	Simonson et al. [124]
512.78 ± 0.02	–	278.3 ± 1.5	Polikhronidi et al. [43]
513.15	7.9540	272.0	Kobe and Lynn, Jr. [125]
512.58	8.0959	272.0	Kudchadker et al. [126]
512.60	8.0959	272.0	Wilhoit and Zwolinski [127]
512.60	8.1035	276.0	IUPAC [22] <sup>a</sup>
512.56	8.0946	269.0	Goodwin [23]
512.60	8.0920	272.0	Smith and Srivastava [128]

Table I. (Continued)

$T_c$ (K)	$P_c$ (MPa)	$\rho_c$ (kg·m <sup>-3</sup> )	References
512.61	8.1030	–	Zubarev et al. [30]
512.60	8.0972	283.0	Craven and de Reuck [129]
512.64	8.0960	–	Bashirov [49]
512.70 ± 0.20	–	267.40	Suleimanov [42]
512.78	8.1000	267.80	Bazaev et al. [7]
512.78 ± 0.02	–	277.49	This work

<sup>a</sup> Recommended values.

### 2.4. Caloric Properties

Except for the data reported by Abdulagatov et al. [4], all previous  $C_V$ – $V$ – $T$  measurements for pure methanol [29,46,47] have been performed at low temperatures (up to 420 K) in the liquid phase with twin calorime-

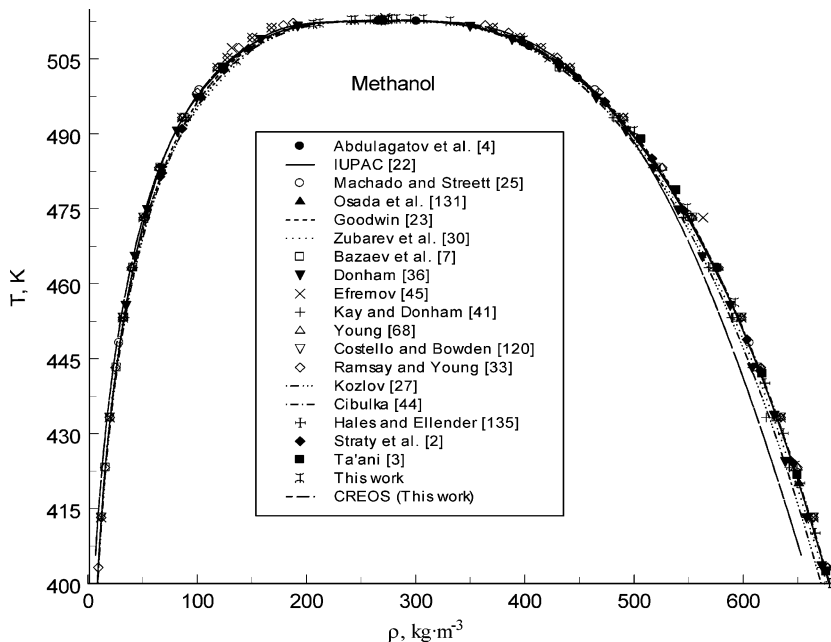


Fig. 3. Experimental saturated-liquid and -vapor densities of methanol in the critical region reported by various authors [2–4, 7, 25, 33, 36, 41, 45, 68, 120, 131, 135] together with values calculated with CREOS97-04 and various correlations developed by other authors [22, 23, 27, 30, 44].

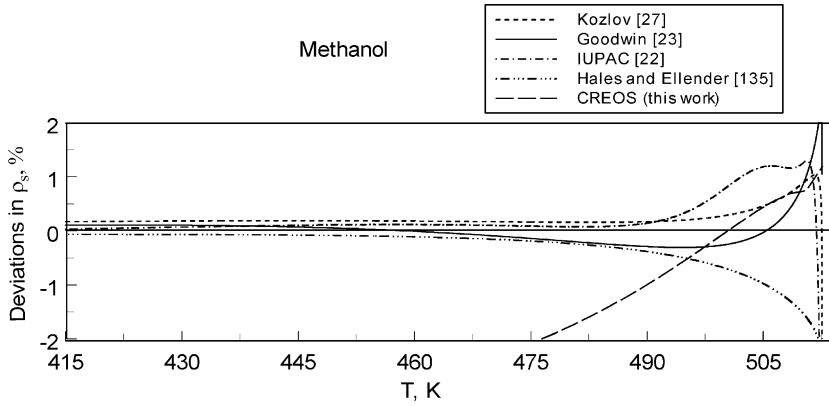


Fig. 4. Comparison of saturated-liquid densities calculated with the correlation by Cibulka [44] with values calculated by CREOS97-04 and correlations proposed by other authors [22, 23, 27, 135].

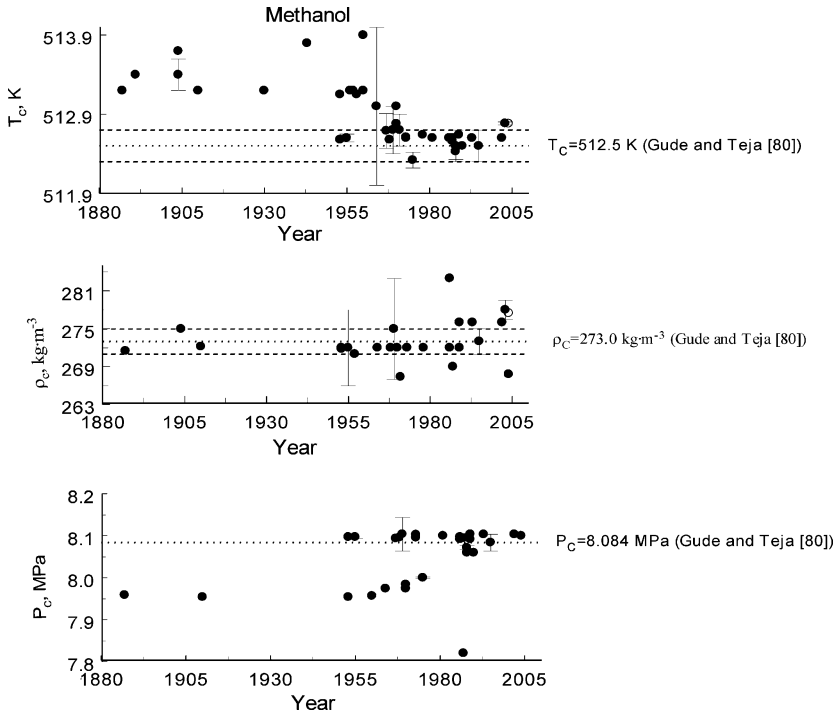


Fig. 5. Distribution of the critical parameters for methanol reported by different authors.

ters, and no isochoric-heat-capacity data were published before 1992. Abdulagatov et al. [4] have reported  $C_V$ - $V$ - $T$  data for methanol (purity of 99.3 mass% with 0.5 mass%  $H_2O$ ) along six isochores in the range from 266 to 449  $kg \cdot m^{-3}$  at temperatures from 443 to 521 K. The uncertainty of the measured heat capacities in the critical region is within 2–3%. After the measurements have been completed, some gases were released from the calorimetric cell and a shift between the saturation temperatures for cooling and heating regimes for each measured density was found. Suleimanov [42] has reported comprehensive measurements of the isochoric heat capacities of pure methanol in the temperature range from 470 to 620 K and densities between 68 and 526  $kg \cdot m^{-3}$ . These temperature and density ranges include single- and two-phase ranges, the coexistence curve, and near- and supercritical ranges. Most measurements were performed near the phase-transition points in order to accurately extract coexistence-curve data ( $T_s - \rho_s$ ) near the critical point. The uncertainty in the heat-capacity measurements is to within 1.5% for the liquid phase and increases up to 5.5% for the vapor phase and in the critical region.

Recently, Polikhronidi et al. [5] have reported new isochoric-heat-capacity measurements for pure methanol in the temperature range from 300 to 556 K and for densities between 136 and 750  $kg \cdot m^{-3}$  including the critical region and along the coexistence curve. Measurements were performed along 14 liquid and eight vapor isochores. A total of 22 values of  $C_V$  at saturation were reported, and the uncertainty of these data in the critical region is 2%.

Except for the five data points at  $P = 8.3$  MPa and at temperatures between 393 and 503 K, obtained by Boyette and Criss [48] who used a high-temperature and high-pressure flow heat-capacity calorimeter, no isobaric-heat-capacity data under pressure were published before 1992. Recently, Bashirov [49] has obtained isobaric-heat-capacity data for pure methanol in the temperature range from 298.15 to 520.65 K and at pressures up to 50 MPa with an impulse method. The uncertainty of these heat-capacity measurements is about 2%.

Yerlett and Wormald [1] have measured of the specific-enthalpy increment  $\Delta H$  of pure methanol in the temperature range from 373 to 573 K at pressures from 0.1 to 13.6 MPa with a flow calorimeter. The uncertainty of the specific enthalpy  $\Delta H$  increment measurements was 0.6%. McCracken and Smith [50] and Lydersen [51] have reported enthalpy data for pure methanol at temperatures up to 573 K and at pressures up to 9.7 MPa. McCracken and Smith [50] used a Freon-11 boil-off calorimeter to obtain data in the range from 394 to 514 K at pressures up to 9.7 MPa with an uncertainty of about 2–3%.

## 2.5. Speed of Sound

Information about the speed of sound in methanol is very scarce. We found only one experimental data set containing speed-of-sound data for pure methanol in the critical region. Akhmetzyanov et al. [52, 53] have measured the speed of sound in the vapor in the critical region with an optical method. The measurements cover a temperature range from 397 to 538 K at pressures up to 10 MPa. Data were obtained at eight vapor densities between 14.93 and 259.74 kg·m<sup>-3</sup>. Sixteen values of the speed of sound of methanol were reported at saturation in the temperature range from 398 to 513 K. The results of the measurements were used to calculate the values for the isobaric and isochoric heat capacities near the critical point. Suleimanov [42] has reported derived values of the speed of sound in pure methanol at saturation near the critical point calculated from experimental isochoric-heat-capacity data. Nozdrev [54] has measured the speed of sound in methanol at saturation near the critical point and has extracted from his measurements values of the critical parameters  $T_c$  and  $\rho_c$ . However, all experimental data were presented only in graphical form.

## 2.6. Critical Parameters

The following methods have been used in the literature to determine the critical parameters of pure methanol:

- (i) Observation of the appearance and disappearance of the vapor–liquid interface (visual method, glass tube or cell with windows) [33, 39, 41, 45, 55–71]
- (ii) Law of rectilinear diameter [33, 41, 45, 60, 62, 68]
- (iii)  $PVT$  relations, (nonvisual)  $(\partial P/\partial V)_T = (\partial^2 P/\partial V^2)_T = 0$ , isothermal and isochoric break methods [7, 31, 37, 64, 66]
- (iv) Acoustic method of determination of the critical point [54]
- (v) Method of quasi-static thermograms (this work, see also Polikhronidi et al. [5])

Most critical property data have been obtained by using a visual method (glass tube or cell with windows). Equilibrium is reached very slowly near the critical point; therefore, it cannot be achieved when the sample under study is unstable and it is necessary to make measurements quickly (low residence time). Decomposition leads to a change in the observed values of the critical parameters with time (see Ambrose and Young [73]). To obtain the correct values of the critical parameters, it is necessary to extrapolate the observations back to a hypothetical zero

time at which the sample could be considered to have been at its critical condition and no decomposition had occurred. The methods for measuring critical parameters of thermally unstable fluids or reactive compounds (flow method; transient pulse-heating thin wire probe) have been proposed by various authors (see, for example, Refs. [74–79]). These methods are capable of residence times between 0.01 ms and 30 s. Unfortunately, these methods have not been applied to the measurement of the critical parameters of methanol. An exception exists for higher molar mass alcohols ( $n > 12$ ) for which Nikitin et al. [77] used a transient pulse-heating thin-wire-probe technique to measure the critical parameters.

Marshall and Jones [71] have measured the vapor–liquid critical temperature of pure methanol and their aqueous mixtures by using a visual method (meniscus separating liquid and vapor phases disappears at equal volumes of the phases). The uncertainty of the measured value of the critical temperature is about 0.4 K. The vapor-liquid critical point of pure methanol (99.5 mol% purity) and of methanol +  $n$ -alkane mixtures were measured visually by de Loos et al. [39] in a high-pressure capillary glass tube apparatus by using a synthetic method. The uncertainty of the critical-temperature measurements is  $\pm 0.05$  K. The critical temperature and critical pressure reported by de Loos et al. [39] agree with the recommended data [80] within 0.2 K and 0.024 MPa, respectively. Bazaev et al. [7] derived values of the critical parameters for methanol from precise  $P$ – $V$ – $T$  measurements using the law of rectilinear diameters. The reported values are  $T_c = 512.78 \pm 0.2$  K,  $\rho_c = 267.8 \pm 2$  kg  $\cdot$  m<sup>3</sup>, and  $P_c = 8.10 \pm 0.02$  MPa.

The experimental method most widely used to measure the coexistence curve near the critical point is by directly observing the appearance and disappearance of the meniscus, but the observations are impeded by development of critical opalescence. This method lacks objectivity. Moreover, as the critical point is approached, the difference between the liquid and vapor phases vanishes, and the visual determination of the moment at which the phase transition occurs becomes even less reliable. Therefore, the region of temperatures approximately  $\pm 1$  K within  $T_c$  becomes virtually inaccessible for investigation (impractical for precise measurements with this method). The method of quasi-static thermograms [72,81–83] makes it possible to obtain reliable data up to temperatures within  $\pm 0.01$  K from  $T_c$  with an uncertainty of  $\pm 0.02$  K (see below).

Gude and Teja [80] have reviewed the critical-property data of pure methanol. They recommended critical-property data ( $T_c = 512.5 \pm 0.2$  K,  $\rho_c = 273 \pm 2$  kg  $\cdot$  m<sup>3</sup>,  $P_c = 8.084 \pm 0.02$  MPa). All available experimental critical parameters data reported in the literature are summarized in Table I and in Fig. 5. In Table I we have also included the values of the critical parameters estimated and recommended by different authors. As one

can see, the available critical temperatures for methanol vary from 505.2 to 536.2 K, critical pressures from 7.065 to 9.701 MPa, and critical densities from 267.4 to 358.7 kg·m<sup>-3</sup>. The difference between the reported values of the critical parameters and values recommended by Gude and Teja [80] lie between -23.7 and 7.3 K, -1.62 to 1.02 MPa, and -85.7 to 4.0 kg·m<sup>-3</sup> for the critical temperature, pressure, and density, respectively. As shown in Fig. 5, the scatter in the critical-temperature measurements is significantly higher than for the critical pressure and critical density.

### 3. ISOCHORIC HEAT-CAPACITY MEASUREMENTS

The experimental apparatus used in this work for measuring isochoric heat capacities for pure methanol in the critical region is the same as that used for other pure fluids (H<sub>2</sub>O, D<sub>2</sub>O, CO<sub>2</sub>, N<sub>2</sub>O<sub>4</sub>, C<sub>6</sub>H<sub>7</sub>), and mixtures (H<sub>2</sub>O + D<sub>2</sub>O, CO<sub>2</sub> + *n*-decane) [43, 72, 82, 84–89]. The apparatus and experimental procedures have been described in previous publications [43, 72, 82, 84–89] and were used without modification. Thus, only a brief discussion will be given here. The isochoric heat capacities were measured with a high-temperature, high-pressure, adiabatic, and nearly constant-volume calorimeter, which yields an uncertainty of 2% in the critical region. The volume of the calorimeter at atmospheric pressure and  $T = 297.15$  K is  $105.126 \pm 0.05$  cm<sup>3</sup>, and is a function of temperature and pressure. The values of the calorimeter volume at a given  $P$  and  $T$  were determined by using  $PVT$  data for pure water (IAPWS standard [90]). The maximum uncertainty in the determination of the volume of the calorimeter at any  $T$  and  $P$  in our experiment is about 0.05%. The mass  $m$  of the sample was measured by using a weighing method with an uncertainty of 0.05 mg. Therefore, the uncertainty in the measurements of density  $\rho = m/V(P, T)$  is about 0.06%. The heat capacity was obtained from the measured  $m$  (mass of the sample),  $\Delta Q$  (amount of electrical energy),  $\Delta T$  (temperature rise resulting from addition of energy  $\Delta Q$ ), and  $C_0$  (empty calorimeter heat capacity). The uncertainty of temperature measurements was less than 15 mK. The heat capacity of the empty calorimeter  $C_0$  was determined experimentally by using a reference fluid (helium-4) with well-known (uncertainty is 0.1%) isobaric heat capacities [91] in the temperature range up to 1000 K at pressures up to 20 MPa. The measured values of empty calorimeter heat capacity  $C_0$  range from 60 to 70 J·K<sup>-1</sup> depending on temperature. The absolute uncertainty in  $C_V$  due to adiabatic losses is 0.013 kJ·K<sup>-1</sup>. The combined standard uncertainty related to the indirect character of the measurements did not exceed 0.16%. Based on a detailed analysis of all sources of uncertainties likely to affect the determination  $C_V$  of with the present system, the combined

standard uncertainty of measuring the heat capacity with allowance for the propagation of error related to the non-isochoric conditions of the process was 2%.

The heat capacity was measured as a function of temperature at nearly constant density. The calorimeter was filled at room temperature, sealed off, and heated along a quasi-isochore. Each experimental run was normally started in the two-phase region and completed in the single-phase region. This method enables one to determine with good accuracy the transition temperature  $T_s$  of the system from the two-phase to a single-phase state (*i.e.*, to determine  $T_s$  and  $\rho_s$  data corresponding to the phase-coexistence curve), the jump in the heat capacity, and reliable data in the single- and two-phase regions (see Polikhronidi et al. [43, 72, 82, 86–89]). The techniques for determining parameters  $T_s$  and  $\rho_s$  and the heat capacity  $C_v$  of the coexisting vapor and liquid phases are similar to the method of quasi-static thermograms as described in detail in previous papers (see Polikhronidi et al. [72, 82] and Kamilov et al. [83]). The method of quasi-static thermograms makes it possible to obtain reliable data up to the critical temperature with an uncertainty of  $\pm 0.02$  K. The purity of the methanol sample was 99.93 mol%. Measurements of the isochoric heat capacity for pure methanol were performed along six (5 liquid and 1 vapor) near-critical densities: 331.59, 306.93, 294.83, 282.43, 277.49, and 274.87 kg·m<sup>-3</sup> in the temperature range from 382 to 533 K. The experimental single-phase and two-phase  $C_V$  data and ( $C_{V1}$ ,  $C_{V2}$ ,  $T_s$ ,  $\rho_s$ ) values on the coexistence curve are given in Tables II and III and in Figs. 6 to 9.

In Fig. 6 we show the temperature dependence of the isochoric heat capacity of methanol along isochores. The density dependence of the measured values of  $C_V$  along selected supercritical isotherms is shown in Fig. 7. The experimental values of liquid and vapor single-phase ( $C'_{V1}$  and  $C''_{V1}$ ) and two-phase ( $C'_{V2}$  and  $C''_{V2}$ ) isochoric heat capacities at coexistence are shown in Figs. 8 and 9. More detailed measurements were made in the critical region and near the phase transition which are very important for an accurate determination of the phase boundary ( $T_s$ ,  $\rho_s$ ) and the critical ( $T_c$ ,  $\rho_c$ ) properties and for the development of a scaled crossover equation of state. The measured values of the saturated densities for methanol in the critical region together with values reported by other authors are shown in Fig. 3. The critical temperature and the critical density extracted from the present measured saturated properties ( $T_s$  and  $\rho_s$ ) in the critical region are  $T_c = 512.78 \pm 0.02$  K and  $\rho_c = 277.49 \pm 2$  kg·m<sup>-3</sup>, which differ from the values recommended by IUPAC [22] by 0.18 K and 1.93 kg·m<sup>-3</sup> (or 0.7%).

**Table II.** Experimental Values of the Single- and Two-Phase Isochoric Heat Capacities of Methanol

$T$ (K)	$C_V$ (kJ·kg <sup>-1</sup> ·K <sup>-1</sup> )	$T$ (K)	$C_V$ (kJ·kg <sup>-1</sup> ·K <sup>-1</sup> )	$T$ (K)	$C_V$ (kJ·kg <sup>-1</sup> ·K <sup>-1</sup> )
$\rho = 331.59 \text{ kg} \cdot \text{m}^{-3}$		$\rho = 306.93 \text{ kg} \cdot \text{m}^{-3}$		$\rho = 294.83 \text{ kg} \cdot \text{m}^{-3}$	
482.149	5.690	489.844	6.170	487.926	6.240
482.640	5.713	489.967	6.178	488.213	6.233
486.004	5.850	490.240	6.189	488.613	6.255
486.177	5.793	492.809	6.340	495.584	6.566
486.312	5.817	493.000	6.358	495.814	6.590
493.955	6.201	493.287	6.349	495.999	6.581
494.146	6.234	493.478	6.353	503.334	7.147
494.336	6.249	493.669	6.364	503.522	7.129
494.527	6.254	497.470	6.587	503.735	7.133
503.546	6.810	497.603	6.590	504.019	7.117
503.735	6.797	497.832	6.627	511.058	8.810
504.019	6.829	503.168	7.055	511.246	8.839
508.245	7.342	503.735	7.115	511.433	8.884
508.417	7.512	503.924	7.136	511.713	9.025
508.826	7.497	504.113	7.157	511.899	9.150
508.973	7.500	504.302	7.149	512.086	9.352
510.145	7.638	504.826	7.840	512.273	9.682
510.238	7.670	509.017	7.883	512.461	10.060
510.425	7.721	509.365	7.955	512.555	10.285
510.705	7.894	511.081	8.700	512.648	10.700
510.892	7.990	511.268	8.765	512.742	11.248
511.174	8.203	511.455	8.815	512.772 <sup>a</sup>	11.603 <sup>a</sup>
511.362	8.287	511.643	8.890	512.772 <sup>a</sup>	6.070 <sup>a</sup>
511.643	8.480	511.874	8.995	512.836	5.983
511.924	8.712	512.057	9.166	512.929	5.796
512.112	8.820	512.245	9.430	513.023	5.644
512.206	8.917	512.339	9.536	513.330	5.467
512.300	9.105	512.433	9.710	513.517	5.322
512.346 <sup>a</sup>	9.156 <sup>a</sup>	512.526	9.938	513.704	5.210
512.346 <sup>a</sup>	5.210 <sup>a</sup>	512.620	10.255	513.892	5.127
512.361	5.213	512.714	10.608	514.080	5.050
512.455	5.110	512.727 <sup>a</sup>	10.673 <sup>a</sup>	518.840	4.389
512.643	4.974	512.727 <sup>a</sup>	5.750 <sup>a</sup>	519.026	4.380
512.768	4.880	512.808	5.589	519.399	4.397
513.049	4.758	512.902	5.485	519.585	4.380
513.142	4.719	512.995	5.408	526.914	4.122
513.330	4.662	513.089	5.320	527.077	4.117
513.518	4.630	513.183	5.258	527.284	4.124
514.082	4.542	513.370	5.151	527.562	4.105
514.364	4.540	513.464	5.165	$\rho = 274.87 \text{ kg} \cdot \text{m}^{-3}$	
514.458	4.588	513.652	5.027	474.392	5.783
516.322	4.355	513.841	4.940	474.559	5.804

Table II. (Continued)

$T$ (K)	$C_V$ (kJ · kg <sup>-1</sup> · K <sup>-1</sup> )	$T$ (K)	$C_V$ (kJ · kg <sup>-1</sup> · K <sup>-1</sup> )	$T$ (K)	$C_V$ (kJ · kg <sup>-1</sup> · K <sup>-1</sup> )
516.613	4.330	574.068	4.880	474.753	5.841
516.895	4.318	514.256	4.810	484.078	6.219
520.947	4.102	518.747	4.353	484.342	6.238
521.259	4.086	519.026	4.340	484.654	6.234
521.538	4.073	519.306	3.324	494.527	6.748
521.724	4.067	519.492	4.333	494.813	6.800
525.712	3.840	525.342	4.088	495.099	6.719
525.897	3.843	525.527	4.086	503.735	7.403
526.082	3.830	525.712	4.098	503.924	7.512
526.267	3.834	525.989	4.060	504.113	7.464
531.160	3.810	$\rho = 277.49$ kg · m <sup>-3</sup>		504.302	7.509
531.248	3.817	381.733	3.460	507.226	8.028
531.614	3.822	381.912	3.465	507.508	7.986
$\rho = 282.43$ kg · m <sup>-3</sup>		382.047	3.459	507.696	7.998
455.700	5.055	392.622	3.608	507.791	7.910
455.899	5.063	392.814	3.622	511.582	9.354
456.098	5.048	392.970	3.615	511.780	9.503
456.297	5.060	413.892	3.940	511.874	9.486
464.603	5.340	414.117	3.937	512.062	9.677
464.699	5.412	414.832	3.968	512.155	9.780
464.808	5.476	435.561	4.513	512.249	9.919
465.079	5.368	435.733	4.497	512.436	10.316
475.170	5.754	435.898	4.493	512.530	10.633
475.364	5.747	454.706	5.060	512.623	11.660
475.559	5.761	454.942	5.054	512.717	11.780
475.851	5.770	455.348	5.079	512.779 <sup>a</sup>	12.780 <sup>a</sup>
484.078	6.140	464.603	5.398	512.779 <sup>a</sup>	6.442 <sup>a</sup>
485.177	6.155	464.719	5.380	512.810	6.410
485.612	6.169	464.998	5.396	512.998	6.119
485.937	6.171	475.948	5.769	513.164	5.844
494.241	6.680	476.120	5.783	513.352	5.680
494.431	6.713	476.343	5.810	513.517	5.598
494.623	6.692	486.004	6.250	513.704	5.400
494.815	6.758	486.317	6.296	513.891	5.317
502.979	7.349	486.642	6.284	514.172	5.220
503.168	7.335	495.576	6.800	514.360	4.980
503.263	7.340	495.732	6.884	514.547	4.900
503.452	7.351	495.944	6.911	518.840	4.490
508.638	8.111	503.169	7.370	519.026	4.524
508.826	8.163	495.944	6.911	519.399	4.533
509.014	8.209	503.169	7.370	519.492	4.472
509.295	8.275	503.170	7.473	527.377	4.119
511.175	9.110	504.208	7.613	527.654	4.169
511.362	9.185	508.826	8.188	527.746	4.090
511.549	9.263	509.130	8.364	528.029	4.113

Table II. (Continued)

$T$ (K)	$C_V$ (kJ·kg <sup>-1</sup> ·K <sup>-1</sup> )	$T$ (K)	$C_V$ (kJ·kg <sup>-1</sup> ·K <sup>-1</sup> )	$T$ (K)	$C_V$ (kJ·kg <sup>-1</sup> ·K <sup>-1</sup> )
511.830	9.399	509.642	8.439	—	—
512.060	9.556	510.693	8.980	—	—
512.247	9.835	511.078	9.164	—	—
512.341	9.990	511.737	9.404	—	—
512.528	10.416	512.300	9.995	—	—
512.620	10.730	512.487	10.355	—	—
512.716	11.364	512.674	11.324	—	—
512.780 <sup>a</sup>	12.705 <sup>a</sup>	512.768	12.970	—	—
512.780 <sup>a</sup>	6.310 <sup>a</sup>	512.785 <sup>a</sup>	13.342 <sup>a</sup>	—	—
512.809	6.206	512.785 <sup>a</sup>	6.440 <sup>a</sup>	—	—
512.903	5.910	512.862	6.328	—	—
512.996	5.596	513.236	5.702	—	—
513.184	5.530	513.423	5.539	—	—
513.562	5.426	513.704	5.394	—	—
513.748	5.324	514.173	5.210	—	—
514.030	5.218	514.361	5.147	—	—
514.216	5.145	516.322	4.830	—	—
514.406	5.088	516.939	4.770	—	—
514.827	5.070	520.051	4.498	—	—
519.306	4.543	520.640	4.463	—	—
519.585	4.520	520.837	4.475	—	—
519.771	4.507	523.766	4.208	—	—
519.864	4.499	524.321	4.188	—	—
526.914	4.093	528.075	4.098	—	—
527.099	4.090	528.940	4.090	—	—
527.284	4.094	532.172	4.064	—	—
527.469	4.098	532.617	4.083	—	—
531.160	4.033	532.843	4.039	—	—
531.630	4.047	532.984	4.030	—	—

<sup>a</sup> Phase transition points

#### 4. THEORETICAL MODELS AND EQUATIONS OF STATE

Thermodynamic modeling of pure methanol at near-critical and super-critical conditions is another important goal of this work. Due to the large scatter in reported thermodynamic and critical properties data for methanol, it is difficult to develop an accurate model for methanol. A brief review of the available theoretical models for methanol and highly associated fluid is given below.

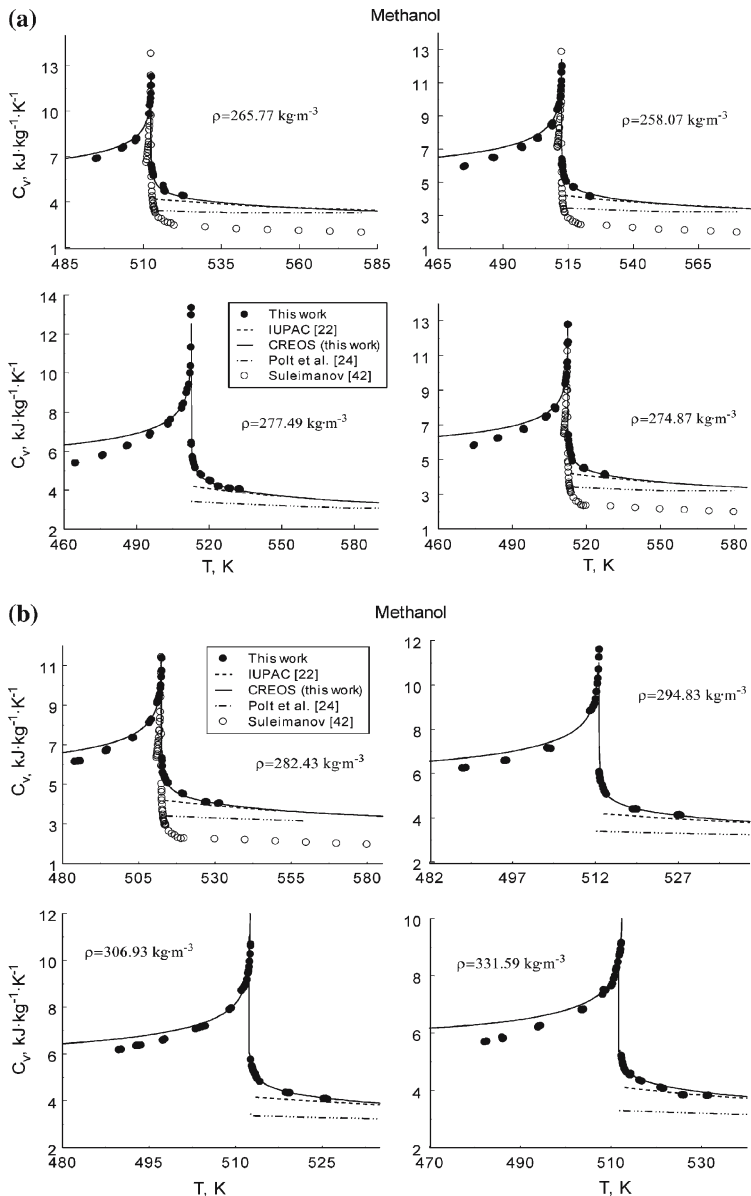


**Fig. 6.** (a, b) Experimental single- and two-phase isochoric heat capacities of methanol as a function of temperature along the near-critical isochores together with values calculated with CREOS97-04 and multiparameter equations of state by IUPAC [22] and by Polt et al. [24].

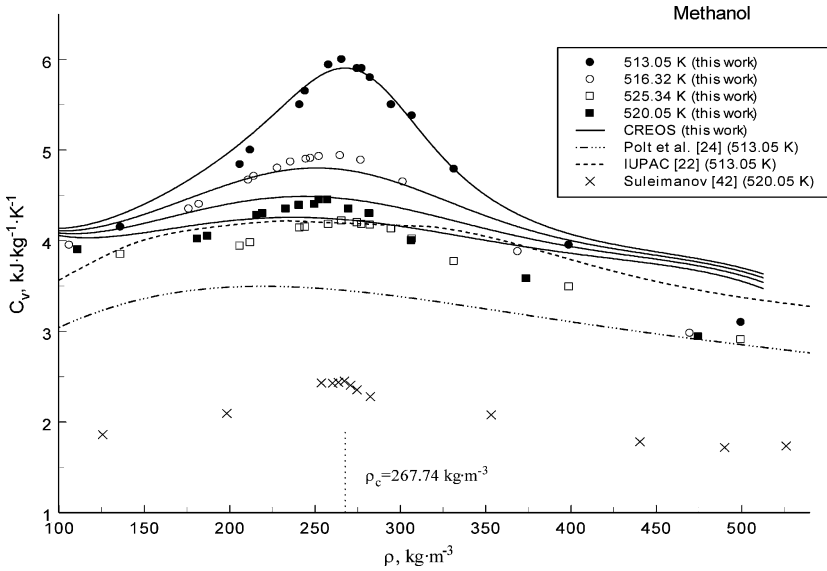


Fig. 7. Experimental single-phase isochoric heat capacities of methanol as a function of density along selected supercritical isotherms together with values calculated with CREOS97-04 and multiparameter equations of state by IUPAC [22] and by Polt et al. [24].

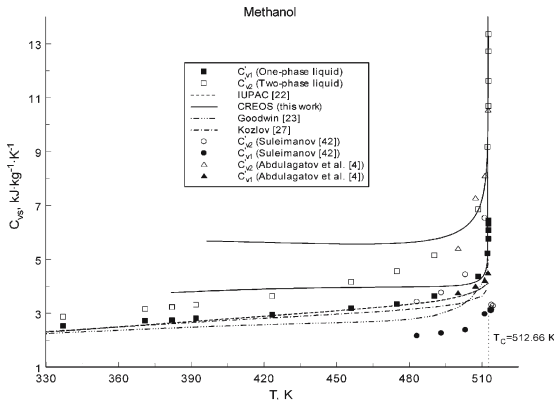


Fig. 8. Experimental single- and two-phase saturated-liquid isochoric heat capacities of methanol as a function of temperature together with values reported by other authors [4, 42] and calculated with CREOS97-04 and multiparameter equations of state developed by other authors [22, 23, 27].

Table III. Isochoric Heat Capacity of Methanol at Saturation

$T_s$ (K)	$\rho'_s$ ( $\text{kg} \cdot \text{m}^{-3}$ )	$C'_{V2}$ ( $\text{kJ} \cdot \text{kg}^{-1} \cdot \text{K}^{-1}$ )	$C'_{V1}$ ( $\text{kJ} \cdot \text{kg}^{-1} \cdot \text{K}^{-1}$ )
512.346	331.59	9.1560	5.210
512.727	306.93	10.673	5.750
512.772	294.83	11.603	6.070
512.780	282.43	12.705	6.310
512.785	277.49	13.342	6.440
$T_s$ (K)	$\rho''_s$ ( $\text{kg} \cdot \text{m}^{-3}$ )	$C''_{V2}$ ( $\text{kJ} \cdot \text{kg}^{-1} \cdot \text{K}^{-1}$ )	$C''_{V1}$ ( $\text{kJ} \cdot \text{kg}^{-1} \cdot \text{K}^{-1}$ )
512.779	274.87	12.780	6.442

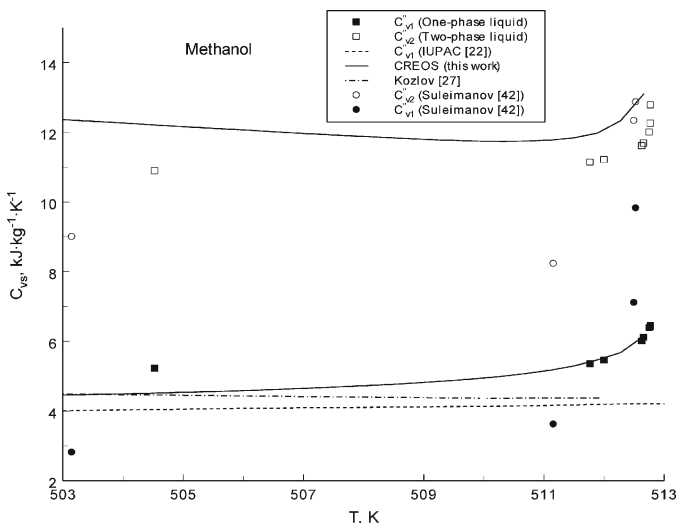


Fig. 9. Experimental single- and two-phase saturated vapor isochoric heat capacities of methanol as a function of temperature together with values reported by other authors and calculated with CREOS97-04 and multiparameter equations of state [22, 23, 27].

### 4.1. Classical Analytical Models

Vlachou et al. [19] have developed an equation of state for systems of fluids interacting with strong specific interactions including hydrogen bonding. This equation has been applied to represent the volumetric properties of water at near-critical and supercritical conditions. The degree of hydrogen bonding at supercritical condition was estimated and compared with the results of NPT molecular-dynamics calculations and with available experimental data. To accurately reproduce the thermodynamic behavior of associating fluids (hydrogen bonding sys-

tems), Economou and Donohue [20] have developed chemical, quasi-chemical, and perturbation (physical) theories that explicitly take into account hydrogen-bonding interactions. It has been shown that all three approaches lead to expressions that are of the same functional form for pure components and for mixtures. Chapman et al. [21] have proposed an equation of state for associated fluids as a sum of three Helmholtz energy terms: Lennard–Jones segment (temperature-dependent hard sphere + dispersion), chain (increment due to chain formation), and association (increment due to association). This equation of state is based on the statistical associating fluid theory (SAFT). The agreement between this model and molecular simulation data is good. The predictive capability of the equation of state is better than that of more empirical equations of state. Recently, Vlček and Nezbeda [92] have developed a simple thermodynamic model and performed computer simulations of associating fluids (ammonia, methanol, ethanol, and water) that descend directly from realistic Hamiltonians and reproduce the structure of real fluids. Analytic expressions for the Helmholtz free energy of methanol have been derived from the thermodynamic perturbation theory, and the effect of the properties of a hydrogen-bonded network on the behavior of different models has been investigated [92].

Due to extreme difficulties of real experimental measurements caused by thermal instability and dissociation–association reactions that appear in fluids such as methanol at high temperatures, computer simulations have become a powerful tool for studying the structure of supercritical hydrogen bonding fluids. Molecular dynamics (MD) and Monte-Carlo (MC) simulations provide insight into hydrogen bonding [93–95] and can be extremely useful for developing a comprehensive theoretical model. Both simulations and experiments are complementary and stimulate each other to provide a reliable physical picture on the molecular level.

## 4.2. Empirical Multiparameter Equations

Thermodynamic properties of pure methanol have been reviewed and compiled extensively under the auspices of IUPAC and reported in the International Thermodynamic Tables of the Fluid State-12 [22], along with a fundamental equation of state for Helmholtz energy. However, this equation for methanol was developed without the accurate  $C_V$ – $V$ – $T$  data generated after 1992, and, therefore, it cannot be applied to the caloric properties of pure methanol in the asymptotic critical and supercritical regions where the thermodynamic properties of methanol, like those of other fluids, exhibit scaling-type critical anomalies.

A Bender-type multiparameter equation of state has been developed by Polt et al. [24]. A polynomial-type equation of state (16-constant equation) has been developed by Machado and Streett [25] and by Zubarev et al. [30]. A non-analytical, but not a scaling-type equation of state for pure methanol has been developed by Goodwin [23]. Eichholz et al. [96] have developed two Gibbs equations (for liquid and vapor phases) for the restricted range of 273–473 K for pressures up to 4 MPa which avoids the difficulties associated with the critical and supercritical regions.

### 4.3. Crossover Models

It is well known that SAFT models [21, 97–99] give a better description for long-chain and associating fluids such as alcohols. However, even this theoretical model is unable to reproduce simultaneously the heat capacities, speed of sound,  $PVT$ , and VLE properties within their experimental accuracy. A fundamental problem appears when one applies any analytical equation of state, molecular-based or empirical, for the prediction of the thermodynamic properties of fluids and fluid mixtures in the critical and supercritical regions. The thermodynamics of a system in the critical region is dominated by the presence of long-range density fluctuations. As a consequence, the thermodynamic surface of fluids exhibits a singularity at the critical point which can be described in terms of non-analytical scaling laws with universal critical exponents and universal scaling functions [100, 101]. All classical, analytical equation of state mentioned above fail to reproduce the singular behavior of fluids and fluid mixtures in the critical and supercritical regions.

For an accurate representation of the near-critical and supercritical thermodynamic behavior of fluids, non-classical crossover models [100, 102–105] should be used. These asymptotic crossover models incorporate scaling laws asymptotically close to the critical point and are transformed into the analytical Landau expansion far away from the critical point. The asymptotic crossover models can reproduce the thermodynamic properties of simple and complex fluids and fluid mixtures in the extended critical region to within their experimental uncertainty. Although they cannot be extrapolated to low densities and do not recover ideal-gas behavior in the limit of zero density ( $\rho \rightarrow 0$ ), they cover a wide range of parameters of state around the critical point and can be effectively used as an auxiliary equation in the critical region for developing so-called “global” crossover models like the crossover SAFT [106, 107], generalized cubic [108], and structure optimized multiparameter EOS [109]. However, for developing and testing of an asymptotic crossover model, one needs accurate  $C_V$ – $V$ – $T$  measurements of pure methanol in the near- and supercritical regions.

## 5. PARAMETRIC CROSSOVER MODEL FOR METHANOL

The experimental data have been used to develop a crossover Helmholtz free energy model for methanol. For this purpose, we have used the parametric crossover model CREOS-97 developed for pure fluids and fluid mixtures by Kiselev [110], as modified subsequently by Kiselev and Rainwater [111, 112]. The Helmholtz free-energy density of a single-component fluid in this model can be written in the parametric form [110–114],

$$\frac{\rho A(T, \rho)}{P_c} = kr^{2-\alpha} R^\alpha(q) \left[ a\Psi_0(\vartheta) + \sum_{i=1}^5 c_i r^{\Delta_i} R^{-\tilde{\Delta}_i}(q) \Psi_i(\vartheta) \right] + \sum_{i=1}^4 \left( A_i + \frac{\rho}{\rho_c} m_i \right) \tau^i - 1, \quad (2)$$

$$\tau = \frac{T - T_c}{T_c} = r(1 - b^2\vartheta), \quad \Delta\rho = \frac{\rho - \rho_c}{\rho_c} = kr^\beta R^{-\beta+1/2}(q)\vartheta + d_1\tau, \quad (3)$$

where  $b^2$  is a universal linear-model parameter [110] and  $k$ ,  $d_1$ ,  $a$ ,  $c_i$ ,  $A_i$ , and  $m_i$  are system-dependent coefficients. The crossover function  $R(q)$  is defined by [112]

$$R(q) = \left( 1 + \frac{q^2 \Delta_0}{1 + q \Delta_0} \right)^{\frac{1}{\tilde{\Delta}_0}}, \quad q = rg \quad (4)$$

where  $g \propto G_i^{-1}$  ( $G_i$  is the Ginzburg number for the fluid of interest [115–118]) and  $\Delta_0$  is a universal constant. The parametric crossover model, defined by Eqs. (2)–(4), contains the following universal constants: the critical exponents  $\alpha$ ,  $\beta$ ,  $\Delta_i$ ,  $\tilde{\Delta}_i$ , and the linear-model parameter. The values of all universal constants are listed in Table IV, and the exact expressions for the universal scaled functions are given in Table V.

The system-dependent parameters  $k$ ,  $d_1$ ,  $a$ ,  $c_i$ , and  $A_i$  for methanol have been found from a fit of Eqs. (2)–(4) to the selected  $PVT$  and  $VLE$  data. As was mentioned above, the available experimental data for the methanol display scatter that is larger than the reported uncertainties. In this work, we selected the data obtained by Straty et al. [2], Bazaev et al. [7], Zubarev and Bagdonas [31], and by Finkelstein and Stiel [32]. In order to provide a better extrapolation of the crossover model into the low-temperature region, we also included in our primary data set a few saturated densities and vapor-pressure data points obtained by Donham [36] at temperatures from  $T = 493$ – $511$  K. The parameters  $m_i$  in Eq.

(2), which determine the background contribution to the isochoric heat capacity

$$\rho C_V^{\text{bg}}(T, \rho) / T = -2(P_c / T_c^2) \times [(A_2 + \rho m_2 / \rho_c) + 3(A_3 + \rho m_3 / \rho_c) \tau + 6(A_4 + \rho m_4 / \rho_c) \tau^2], \quad (5)$$

have been found from a fit of the crossover model to the present  $C_V$ - $V$ - $T$  measurements that cover the range of densities between 274.87 and 331.59 kg · m<sup>-3</sup> and temperatures from 495 to 533 K. To extend the range of description of the isochoric heat capacity to higher temperatures, we have also used a few  $C_V$ -data points generated from the IUPAC [22] in the temperature interval between 560 and 620 K. The optimization procedure was performed in three steps. First, we optimized the crossover model to the experimental data in the interval of densities and temperatures bounded by

$$\tau + 2.4\Delta\rho^2 = 1; \quad T \geq 0.995T_c \quad (6)$$

Table IV. Universal Constants

$\alpha = 0.110$	$\tilde{\Delta}_3 = \tilde{\Delta}_4 = \Delta_3 - 0.5 = 0.065$
$\beta = 0.325$	$\tilde{\Delta}_5 = \Delta_5 - 0.5 = 0.69$
$\gamma = 2 - \alpha - 2\beta = 1.24$	$e_0 = 2\gamma + 3\beta - 1 = 2.455$
$b^2 = (\lambda - 2\beta) / \gamma (1 - 2\beta) \cong 1.359$	$e_1 = (5 - 2e_0)(e_0 - \beta)(2e_0 - 3) / 3(e_0 - 5\beta) \cong 0.147$
$\Delta_1 = \tilde{\Delta}_1 = 0.51$	$e_2 = (5 - 2e_0)(e_0 - 3\beta) / 3(e_0 - 5\beta) \cong 5.35 \cdot 10^{-2}$
$\Delta_2 = \tilde{\Delta}_2 = 2\Delta_1 = 1.02$	$e_3 = 2 - \alpha - \Delta_5 = 3.08$
$\Delta_3 = \Delta_4 = \gamma + \beta - 1 = 0.565$	$e_4 = (2e_3 - 5)(e_3 - 3\beta) / 3(e_3 - 5\beta) \cong 0.559$
$\Delta_5 = 1.19$	$\Delta_0 = 0.5$

Table V. Universal Scaled Functions

$\Psi_0(\vartheta) = \frac{1}{2b^4} \left[ \frac{2\beta(b^2-1)}{2-\alpha} + \frac{2\beta(2\gamma-1)}{\gamma(1-\alpha)} (1-b^2\vartheta^2) - \frac{(1-2\beta)}{\alpha} (1-b^2\vartheta^2)^2 \right]$
$\Psi_1(\vartheta) = \frac{1}{2b^2(1-\alpha+\Delta_1)} \left[ \frac{\gamma+\Delta_1}{2-\alpha+\Delta_1} - (1-2\beta)b^2\vartheta^2 \right]$
$\Psi_2(\vartheta) = \frac{1}{2b^2(1-\alpha+\Delta_2)} \left[ \frac{\gamma+\Delta_2}{2-\alpha+\Delta_2} - (1-2\beta)b^2\vartheta^2 \right]$
$\Psi_3(\vartheta) = \vartheta - \frac{2}{3}(e_0 - \beta)b^2\vartheta^3 + \frac{e_1(1-2\beta)}{(5-2e_0)}b^4\vartheta^5$
$\Psi_4(\vartheta) = \frac{1}{3}b^2\vartheta^3 - \frac{e_2(1-2\beta)}{(5-2e_0)}b^4\vartheta^5$
$\Psi_5(\vartheta) = \frac{1}{3}b^2\vartheta^3 - \frac{e_4(1-2\beta)}{(2e_3-5)}b^4\vartheta^5$

**Table VI.** System-Dependent Parameters of the CREOS97-04 Model for Methanol

Parameter	
$a$	$2.71272167 \times 10$
$k$	1.49176163
$c_1$	-4.37159943
$c_2$	$3.26669608 \times 10$
$c_3$	$3.26669608 \times 10$
$c_4$	$1.46834395 \times 10$
$g$	$6.09927217 \times 10^{-3}$
$d_1$	-1.16903429
$A_1$	-9.08467784
$A_2$	$1.47688002 \times 10$
$A_3$	9.77989178
$m_2$	$-2.15121631 \times 10$
$m_3$	$2.81986109 \times 10$
$m_4$	$-1.00077831 \times 10$

with the critical parameters extracted from the  $C_V$  measurements. In the second step, the critical parameters,

$$T_c = 512.660 \text{ K}, \quad \rho_c = 276.74 \text{ kg} \cdot \text{m}^{-3}, \quad P_c = 8.130 \text{ MPa}, \quad (7)$$

have been found from a fit of the crossover model to the experimental data in the asymptotic critical region at  $|\Delta\rho| \leq 0.25$  and  $|\tau| \leq 0.05$ , with the values of the coefficients  $c_i$ ,  $A_i$ , and  $m_i$  ( $i > 2$ ) obtained from the previous fit. And finally, the parameters  $c_i$ ,  $A_i$ , and  $m_i$  ( $i > 2$ ) have been redefined from a fit of the crossover model with the fixed values of the critical parameters, Eq. (7), to the experimental data in the entire density and temperature interval given by Eq. (6). The system-dependent parameters in the Helmholtz free-energy crossover model CREOS97-04 for methanol given by Eqs. (2)–(4) are listed in Table VI.

## 6. RESULTS AND DISCUSSION

The deviations between the saturated pressures calculated with the Ambrose and Walton [34] correlation and values calculated with CREOS97-04 and other correlations are shown in Fig. 2. As one can see, the CREOS97-04 model reproduces all available experimental vapor-pressure data in the critical region with an AAD that is comparable with empirical correlation mentioned above *i.e.*, the model reproduces experimental vapor-pressure data as well as multi-parameter empirical correlations

which were directly fitted to the experimental data. At temperatures up to 490 K, which are outside the range given by Eq. (6), the more reliably secondary saturated pressure data are represented with an uncertainty of about  $\pm 0.75\%$ , while at temperatures above 490 K (but still outside the range of the model) the data are represented within 0.19%. In the temperature range from 460 to the critical temperature, the average absolute deviation (AAD) for all of the vapor-pressure data sets (57 data points) is about 0.34%. The data of Bazev et al. [7] are also represented well, to within about 0.12% at a 95% confidence level. The CREOS97-04 model represents the data of Ambrose et al. [40], Skaates and Kay [38], de Loos et al. [39], and Straty et al. [2] generally within 0.15%, with several outliers at low temperatures (below 483 K). The data of Young [68] are consistently 2.2% lower than the values from the model and other reported data. Differences are up to 0.6–1.4% for the data of Lydersen and Tsochev [37] at temperatures below 493 K and about 0.22% in the critical region.

A comparison of the present saturated density data with values calculated with the CREOS97-04 model in the critical region of methanol together with the secondary data sets reported by different authors is shown in Fig. 3. Most of the data points presented in Fig. 3 lie far below the minimum temperature defined by Eq. (6) ( $T < 502$  K), but nevertheless the CREOS97-04 gives a good representation of these data. In Fig. 4 we show the deviations between the calculated values of the saturated liquid densities with the correlation by Cibulka [44] and values calculated with the CREOS97-04 model, as well with other correlations. As one can see, the percent deviations of the reliable secondary data generated with Cibulka's correlation [44] from the present crossover model are almost the same as ones for the multiparameter equations of state. The model represents the saturated liquid data sets in the entire temperature range from 470 K to the critical point, which is much wider than the range of validity of the crossover model ( $502 \text{ K} < T < T_c$ ), with an AAD of about 0.66%. The data of Donham [36] and Bazaev et al. [7] provide a good test of the extrapolation abilities of the model. In the temperature range where the model is valid, Eq. (6), the deviation are within  $\pm 1.0\%$  (AAD = 0.38%). The data of Donham [36] are generally within  $\pm 1.3\%$  (AAD = 0.78%) of the model. Differences are up to 5–8% for the data of Ramsay and Young [33] and Efremov [45] and 0.93% for the data of Bazaev et al. [7]. The present saturated liquid density data are reproduced with the CREOS97-04 model within 0.78%.

The measured values of single- and two-phase isochoric heat capacities for methanol along the separate isochores and isotherms together with the values calculated with different equations of state are shown in Figs. 6–9. As one can see from Figs. 6 and 7, at low ( $\rho < 150 \text{ kg} \cdot \text{m}^{-3}$ ) and high

densities ( $\rho > 350 \text{ kg} \cdot \text{m}^{-3}$ ) the deviations between  $C_V$  data and values calculated with IUPAC [22] are of about 2–4%, while in the critical region the deviations are increased up to 50%. The values of  $C_V$  calculated with the equation of state developed by Polt et al. [24] lie about 25% lower than the IUPAC [22] predictions and the present results. Excellent agreement between the isochoric heat capacity data and values calculated with CREOS97-04 is observed.

In Figs. 8 and 9 we show the experimental single- and two-phase saturated liquid isochoric-heat-capacity data for methanol in comparison with calculated values. Far from the critical point, in the range where the heat capacity exhibits a regular-analytical behavior, good agreement between present  $C'_{V1}$  data and the values calculated with IUPAC [22], Goodwin [23], and Kozlov [27] equations of state is observed. The IUPAC [22] equation of state represents the present  $C'_{V1}$  data in the temperature range from 337 to 490 K within 2–3%, while at high temperatures ( $T > 490 \text{ K}$ , near the critical temperature), the deviations increase to 11–30%. It is not surprising that the IUPAC [22], Goodwin [23], and Kozlov [27] equations of state cannot even qualitatively reproduce the critical behavior of  $C_V$  near the phase transition temperature and in the critical region (see Figs. 6–9). This is a general shortcoming of all analytical multiparameter equations of state. Large deviations up to 25% and 11% are observed between the present vapor phase  $C''_{V1}$  data and the values calculated with IUPAC [22] and Kozlov [27] equations of state, respectively, in the range far from the critical point ( $T < 505 \text{ K}$ ). Good consistency was found between the present isochoric heat-capacity measurements  $C'_{V1}$  and data reported in an earlier paper by Abdulagatov et al. [4].

The solid curves in Figs. 6–9 correspond to the values of the isochoric heat capacities calculated in the sub- and supercritical regions with the CREOS97-04 model. As one can see, in contrast to the analytical equations of state by IUPAC [22], by Polt et al. [24], and by Kozlov [27], the crossover model reproduces the critical anomaly of  $C_V$  in the near-critical region with high accuracy. The model represents all of the present isochoric heat capacity data points to within  $\pm 3.0\%$  at temperatures above 512 K (in the supercritical region). The AAD = 1.29% for all  $C_VVT$  data presented in Figs. 6–9.

In Figs. 6–9 we also compare the present  $C_V$  data with the values reported earlier by Suleimanov [42]. The deviations of saturated density reported by Suleimanov [42] are within 1–5%, but as one can see from Fig. 3 the regular background part of  $C_V$  data reported by Suleimanov [42] displays an offset of about twice the present values. We assume that this is due to calorimeter calibration issues. We found that after the corresponding shift of the background part, excellent agreement (within 2.2%, which

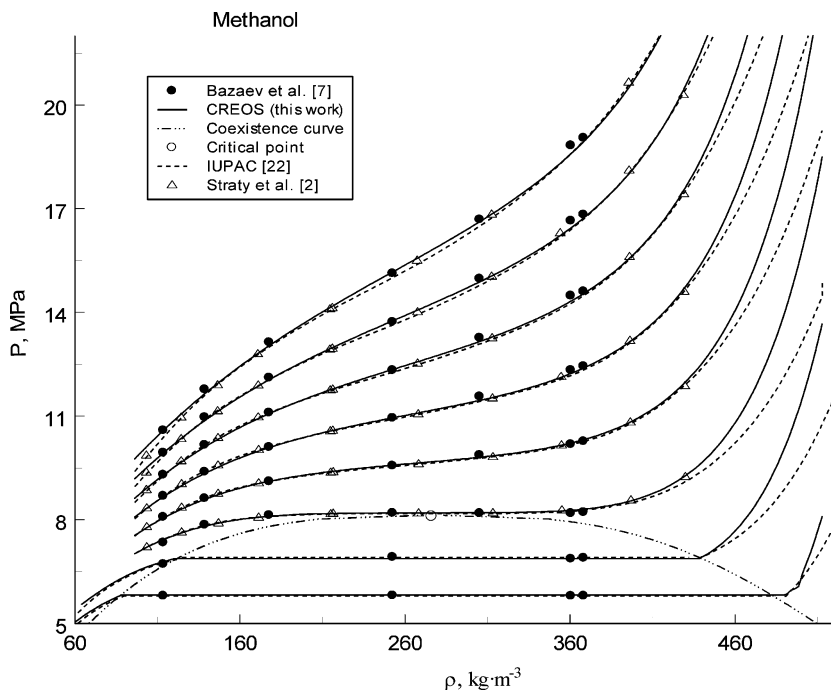
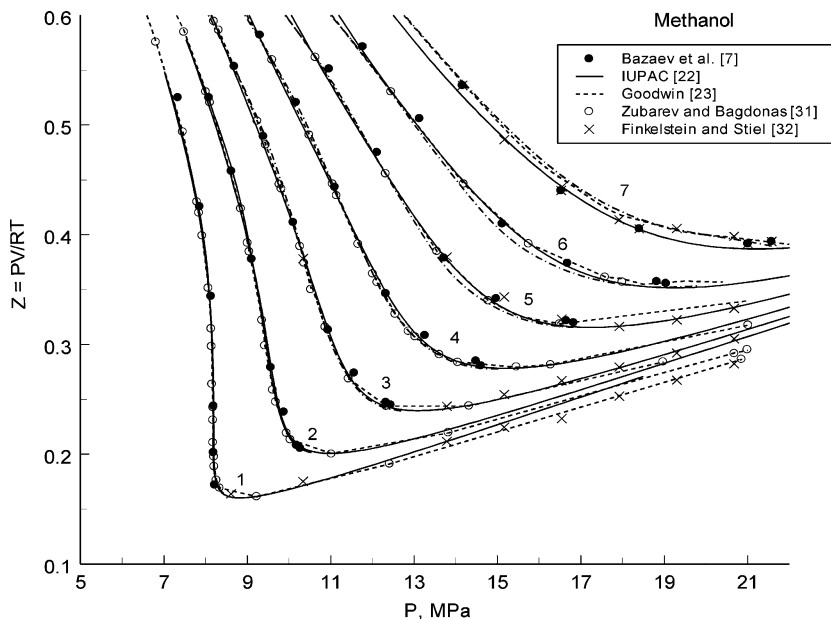


Fig. 10. Experimental  $P - \rho$  dependence of methanol along the near-critical and supercritical isotherms together with values calculated with CREOS97-04 and IUPAC [22].

is very close to their experimental uncertainty of 2.0%) between Suleimanov's [42] data and the present  $C_V$  measurements is observed.

In Figs. 10 and 11, we compare the primary  $PVT$  data sets for pure methanol with values calculated in the sub- and supercritical regions with CREOS97-04. These figures also contain the values of pressure and compressibility factor,  $Z = PV/(RT)$ , calculated with the multiparameter fundamental equations of state (IUPAC [22] and Goodwin [23]). CREOS97-04 reproduces the  $PVT$  data of Bazaev et al. [7] with  $AAD = 0.63\%$  and the data of Straty et al. [2] with  $AAD = 0.37\%$ , although their estimated experimental uncertainty is 0.2%. The data by Zubarev and Bagdonas [31] are represented with an  $AAD = 0.26\%$ , that is within their estimated uncertainty of 0.2–0.3%.

Comparisons of the enthalpy increments,  $\Delta H$ , calculated with CREOS97-04 and the analytical multiparameter IUPAC [22] equation with experimental data reported by Yerlett and Wormald are shown in Figs. 12 and 13. As one can see, in the liquid phase and supercritical region,



**Fig. 11.** Comparison of selected experimental compressibility factors ( $Z = PV/(RT)$ ) reported by different authors [7, 31, 32] for methanol with values calculated with CREOS and multiparameter equations of state by IUPAC [22] and by Goodwin [23].

agreement between calculated values of enthalpy difference and experimental data for both equations is good. The experimental and calculated values of the enthalpy increments  $\Delta H$  along the saturation curve in methanol are shown in Fig. 13. As one can see, down to the temperature  $T = 448\text{ K}$ , both the IUPAC [22] and CREOS97-04 equations reproduce experimental  $\Delta H$  data to within 0.78%, which is close to the experimental uncertainty ( $\sim 0.6\%$ ). Since all secondary data shown in Fig. 13 have not been used in the optimization of the crossover model and most of them lie outside the temperature interval given by Eq. (6), this result indicates the predictive capability of the CREOS97-04 at low temperatures.

The pressure dependence of the calculated isobaric heat-capacity  $C_P$  of methanol along various near- and supercritical isotherms is shown in Fig. 14 together with experimental data obtained by Bashirov [49]. Figure 15 shows the pressure dependence of the isobaric heat capacity of methanol along selected isotherms derived from the speed-of-sound measurements by Akhmetzyanov et al. [52, 53] together with values calculated with CREOS97-04 and IUPAC [22]. As one can see, good agreement between both models and experimental data is observed. However, the val-

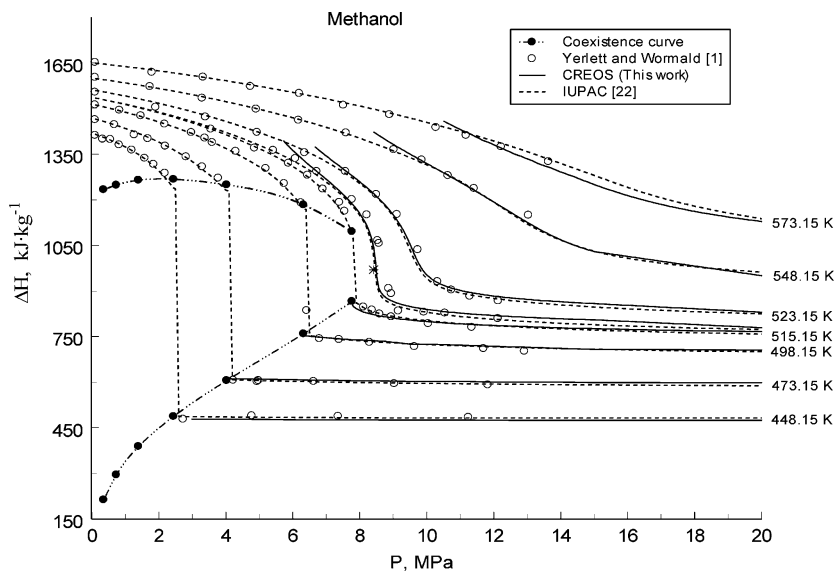


Fig. 12. Experimental enthalpy increments,  $\Delta H$ , reported by Yerlett and Wormald [1] as a function of pressure together with values calculated with CREOS97-04 and IUPAC[22].

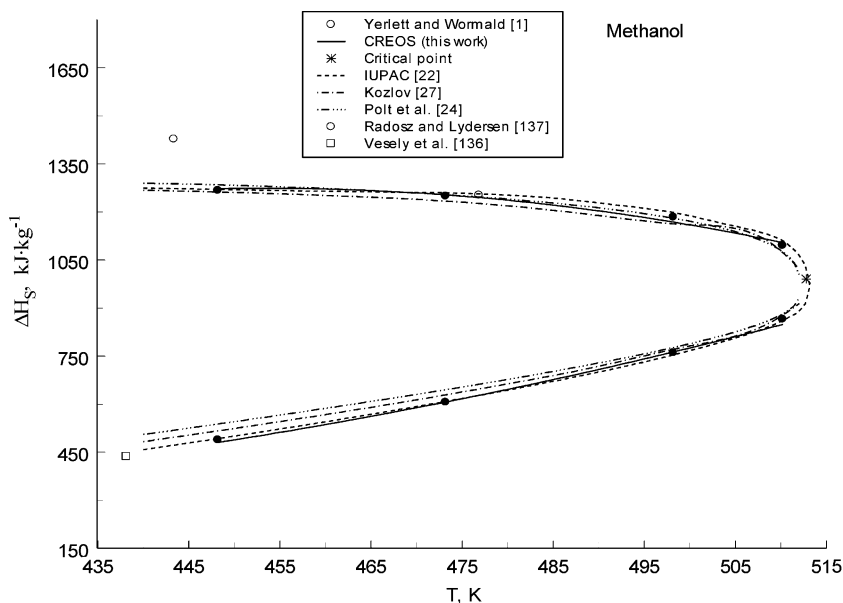
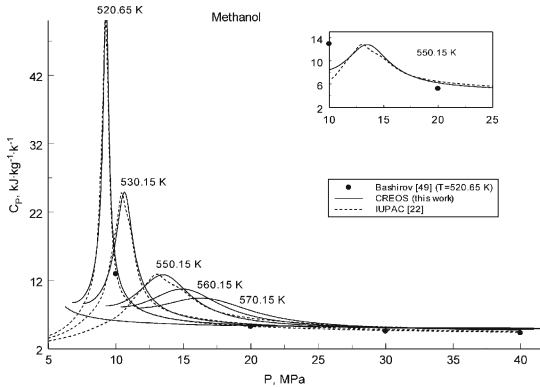
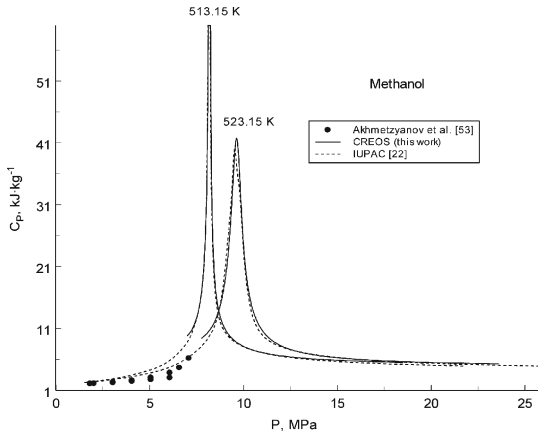


Fig. 13. Experimental enthalpy differences along the saturation curves by different authors [1, 136, 137] together with values calculated with CREOS97-04 and multiparameter equations of state developed by other authors [22, 24, 27].



**Fig. 14.** Comparison of isobaric heat capacities data obtained at selected near-critical and supercritical isotherms by Bashirov [49] with values calculated with CREOS97-04 and IUPAC [22].



**Fig. 15.** Comparison of the isobaric heat capacities derived along two selected supercritical isotherms from the speed-of-sound measurements by Akhmetzyanov [52] with values calculated with CREOS97-04 and IUPAC [22].

ues calculated with IUPAC [22] exhibit some nonmonotonic behavior at near-critical temperatures at pressures near the maximum of  $C_P$ , which are not seen in the CREOS97-04 predictions (see inset in Fig. 14).

In Figs. 16 and 17 we show the comparisons between values of the speed of sound in methanol calculated with various equations of state in the critical and supercritical regions and at saturation (CREOS97-04, IUPAC [22], and Polt et al. [24]). The experimental data were reported by Akhmetzyanov et al. [52, 53]. As one can see from Fig. 16,

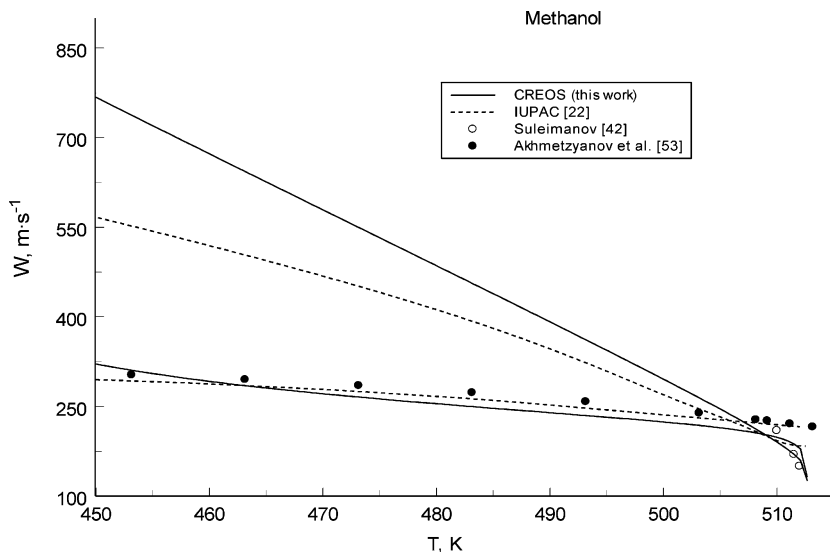
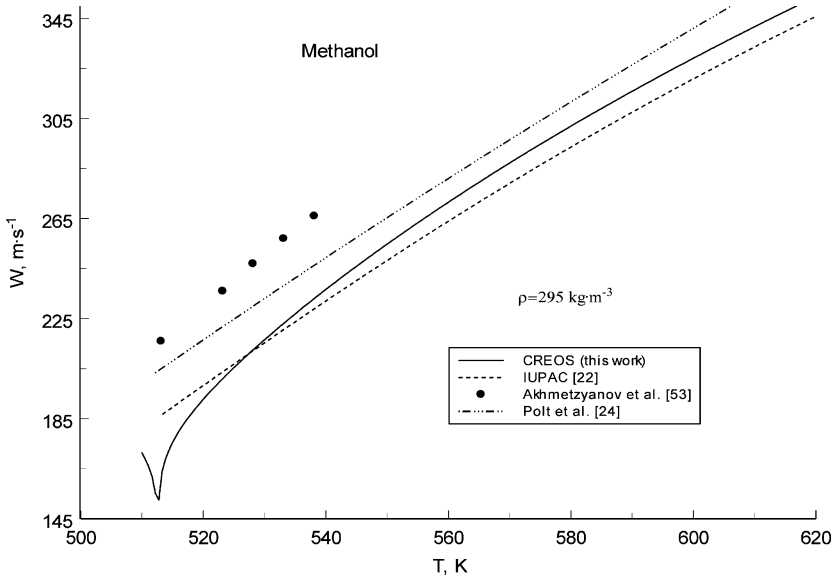


Fig. 16. Comparison of the temperature dependence of speed-of-sound data along the saturation curve in methanol reported by Akhmetzyanov [52] and by Suleimanov [42] with values calculated with CREOS97-04 and IUPAC [22].

the speed-of-sound data also demonstrate excellent extrapolation capability of the present crossover model to low temperatures, up to 450 K. Three data points reported by Suleimanov [42] near the critical point are also very well represented by the model, while the data by Akhmetzyanov et al. [52, 53] lie between 1.0 and 1.5% above the model. These larger deviations between experimental data and values calculated with the crossover model and multiparameter equations of state are also observed on the near-critical isochore of  $259 \text{ kg} \cdot \text{m}^{-3}$ . As shown in Fig. 17, the data reported by Akhmetzyanov et al. [52, 53] lie about 15–20% higher than values predicted by the crossover model. The density dependence of the speed of sound in methanol calculated with the crossover model and from IUPAC [22] and Polt et al. [24] equations of state along the supercritical isotherm at 513.15 K is shown in Fig. 18. Figure 18 also includes the data derived by Akhmetzyanov et al. [52, 53]. As one can see again, the IUPAC [22] predictions exhibit a physically unattractive nonmonotonic behavior, which is not observed for other equations of state.

Deviation plots for the various thermodynamic properties (single-phase pressure, vapor pressures and saturation densities, enthalpies, and isochoric heat capacities) between experimental data sets and calculated



**Fig. 17.** Comparison of the temperature dependence of the speed-of-sound data in methanol along the selected supercritical isochore reported by Akhmetzyanov [52] with values calculated with CREOS97-04 and by IUPAC [22] and by Polt et al. [24].

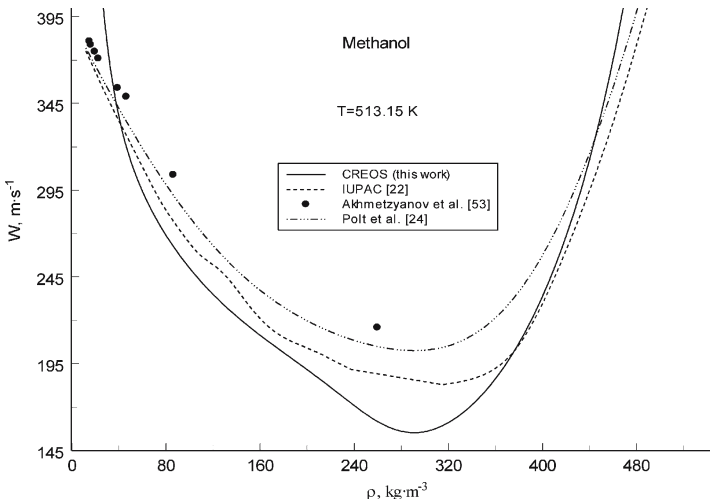


**Fig. 18.** Comparison of density dependence of the speed of sound in methanol selected along isotherm  $T = 513.15 \text{ K}$  reported by Akhmetzyanov [52] and values calculated with CREOS97-04 and multiparameter equations of state by IUPAC [22] and by Polt et al. [24].

with present crossover model are shown in Figs. 19–23 and the deviation statistics for these data is given in Table VII.

**Table VII.** Deviation Statistics (in %) for the CREOS97-04 Model for Methanol

Property	Reference	AAD	Bias	St. Dev.	St. Err.	Max. Dev.	<i>N</i>
<i>PVT</i>	Bazaev et al. [7]	0.63	0.25	0.71	0.07	1.42	100
<i>PVT</i>	Straty et al. [2]	0.37	−0.06	0.47	0.05	1.39	72
<i>PVT</i>	Zubarev and Bagdonas [31]	0.26	0.00	0.32	0.04	0.65	65
$P_s$	Ambrose and Sprake [130]	0.34	0.24	0.48	0.06	1.5	57
$\rho_{v,L}$	Dohman [36]	0.66	−0.02	0.85	0.16	1.48	30
	Ambrose and Sprake [130]	0.78	0.02	0.95	0.14	1.2	45
Enthalpy	Yerlett and Wormald [1]	1.29	0.13	1.48	0.14	2.93	115
$C_V VT$	This work						

## 7. CONCLUSION

New measurements of the isochoric heat capacity of pure methanol in the temperature range from 482 to 533 K, at near-critical liquid and vapor densities between 274.87 and 331.59 kg·m<sup>−3</sup> obtained by using a high-temperature and high-pressure nearly constant-volume adiabatic calorimeter were performed. These data together with recent high accuracy *P–V–T* data reported by other researchers were used to develop a thermodynamically self-consistent crossover equation of state in the critical and supercritical regions. The accuracy of the crossover model was confirmed by a comprehensive comparison with available experimental data for pure methanol and values calculated with various multiparameter equations of state and correlations. At densities 95 kg·m<sup>−3</sup> ≤  $\rho$  ≤ 455 kg·m<sup>−3</sup> and temperatures 500 K ≤ *T* ≤ 650 K the crossover model represents all available experimental thermodynamic properties of pure methanol in the critical and supercritical regions with an accuracy that is very close to their experimental uncertainties. The program CREOS97-04 for the calculation of thermodynamic properties of methanol in the critical region can be obtained from the corresponding author upon request.

## ACKNOWLEDGMENTS

The research in the Institute for Geothermal Problems of the Dagestan Scientific Center of RAS was supported by the Russian Fund of

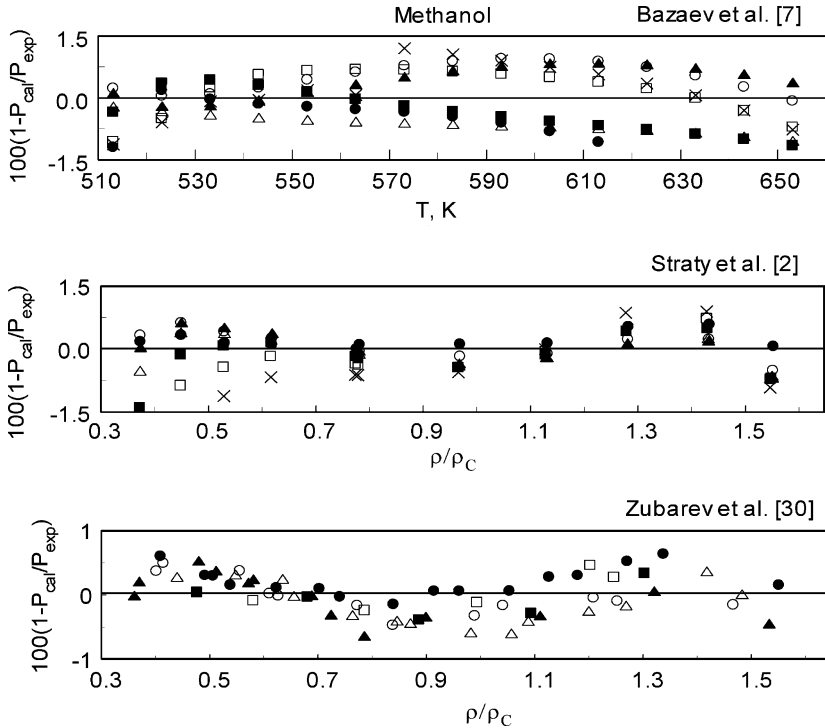


**Fig. 19.** Percentage pressure deviations,  $\delta P = 100(P_{\text{exp}} - P_{\text{cal}})/P_{\text{exp}}$ , of the experimental pressures for methanol reported by various authors from the values calculated with CREOS97-04 as a function of temperature. Bazaev et al. [7]: ●, 3.541 mol·L<sup>-1</sup>; ○, 4.327 mol·L<sup>-1</sup>; ■, 5.545 mol·L<sup>-1</sup>; △, 7.877 mol·L<sup>-1</sup>; ▩, 9.526 mol·L<sup>-1</sup>; □, 11.254 mol·L<sup>-1</sup>; ×, 11.487 mol·L<sup>-1</sup>, Straty et al. [2]: ●, 513.15 K; ×, 523.15 K; ▲, 533.15 K; △, 543.15 K; □, 553.15 K; ▩, 563.15 K; ×, 573.15 K, Zubarev et al. [30]: ●, 513.15 K; ○, 523.15 K; ▲, 533.15 K; △, 543.15 K; ▩, 553.15 K; □, 563.15 K.

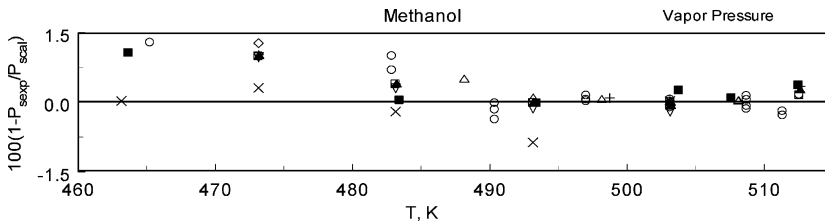


**Fig. 20.** Percentage vapor-pressure deviations,  $\delta P_S = 100(P_{S \text{ exp}} - P_{S \text{ cal}})/P_{S \text{ exp}}$ , of the experimental vapor pressures for methanol reported by various authors from values calculated with CREOS as a function of density. ○, Dohman [36]; ▽, Bazaev [7]; ■, de Loos et al. [39]; ◇, Machado and Streett [25]; △, Straty et al. [2]; +, Ambrose et al. [40]; ▲, Skaates and Kay [38]; ×, Efremov [45]; ▩, Kay and Dohman [41].

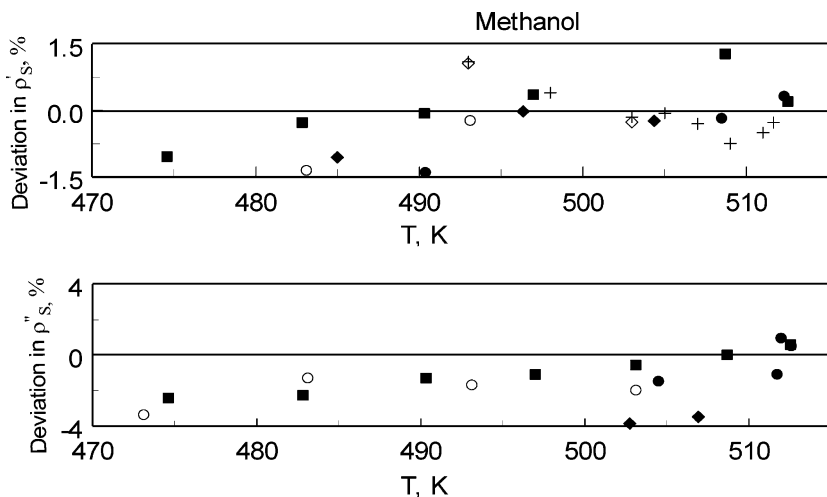


**Fig. 21.** Saturated liquid and vapor density deviations,  $\delta\rho_S = 100(\rho_{\text{sexp}} - \rho_{\text{sca}})/\rho_{\text{sexp}}$ , of the experimental saturated densities for methanol reported by various authors from values calculated with CREOS97-04 as a function of temperature. ●, this work; ○, Bazaev [7]; ■, Dohman [36]; ◇, Suleimanov [42]; ◇, Straty et al. [2]; +, Ramsay and Young [33].

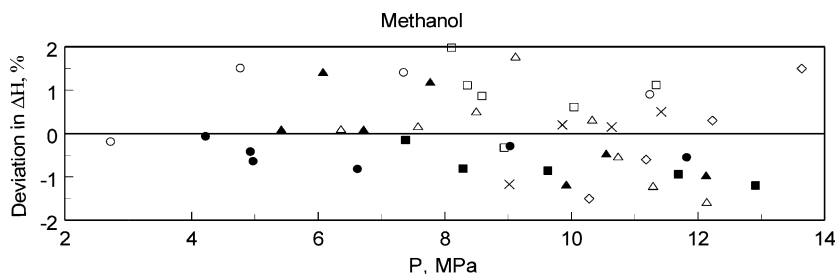


**Fig. 22.** Enthalpy difference deviations,  $\delta\Delta H = 100(\Delta H_{\text{exp}} - \Delta H_{\text{cal}})/\Delta H_{\text{exp}}$ , of the experimental enthalpies for methanol reported by Yerlett and Wormald [1] from values calculated with CREOS97-04 as a function of pressure. ○, 448.15 K; ●, 473.15 K; ■, 498.15 K; □, 510.15 K; ▲, 515.15 K; △, 523.15 K; ×, 548.15 K; ◇, 573.15 K.

Basic Researches under Grant No. RFBR 03-02-16220. The research in the Colorado School of Mines was supported by the U.S. Department of Energy, Office of Basic Energy Sciences, under Grant No. DE-FG03-95ER14568. One of us (I.M.A.) thanks the Physical and Chemical Properties Division at the National Institute of Standards and Technology for the opportunity to work as a Guest Researcher at NIST during the course of this research.

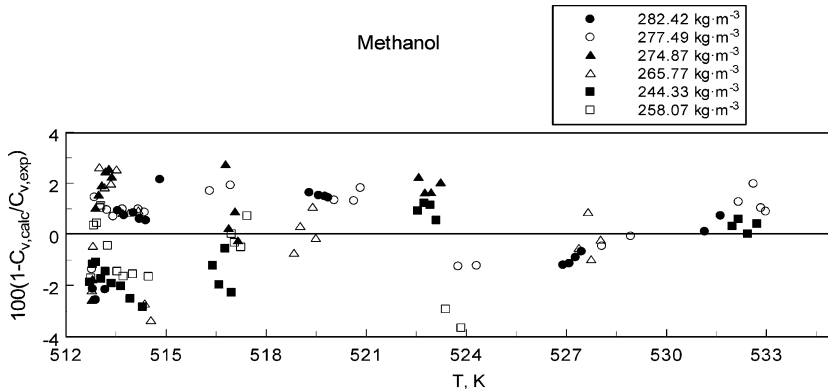


**Fig. 23.** Isochoric heat-capacity deviations,  $\delta C_v = 100(C_{v, \text{exp}} - C_{v, \text{calc}})/C_{v, \text{exp}}$ , of the experimental results for methanol reported in this work from values calculated with CRE-OS97-04 as a function of temperature.

## REFERENCES

1. T. K. Yerlett and C. J. Wormald, *J. Chem. Thermodyn.* **18**:719 (1986).
2. G. C. Straty, A. M. F. Palavra, and T. J. Bruno, *Int. J. Thermophys.* **7**:1077 (1986).
3. R. Ta'ani, Thesis, *Dr. Ing. Thesis* (Karlsruhe, 1976).
4. I. M. Abdulagatov, V. I. Dvorynchikov, M. M. Aliev, and A. N. Kamalov, in *Steam, Water, and Hydrothermal Systems, Proc. of the 13th Int. Conf. on the Props. of Water and Steam* (NRC Research Press., Ottawa, 2000), p. 157.
5. N. G. Polikhronidi, I. M. Abdulagatov, J. W. Magee, G. V. Stepanov, and R. G. Batyrova, to be submitted to *Int. J. Thermophys.*
6. T. J. Bruno and G. C. Straty, *J. Res. Natl. Bur. Stand.* **91**:135 (1986).
7. A. R. Bazaev, I. M. Abdulagatov, J. W. Magee, and E. A. Bazaev, to be submitted to *Int. J. Thermophys.*
8. R. Nakayama and K. Shinoda, *J. Chem. Thermodyn.* **3**:401 (1971).
9. V. P. Belousov and M. Y. Panov, *Thermodynamics of the Nonelectrolyte Aqueous Solutions* (Chemistry, Leningrad, 1983).
10. S. Y. Noskov, M. G. Kiselev, and A. M. Kolker, *Russ. J. Structural Chem.* **40**:304 (1999).
11. S. S. T. Ting, S. J. Macnaughton, D. L. Tomasko, and N. R. Foster, *Ind. Eng. Chem. Res.* **32**:1471 (1993).
12. G. S. Gurdial, S. J. Macnaughton, D. L. Tomasko, and N. R. Foster, *Ind. Eng. Chem. Res.* **32**:1488 (1993).
13. J. M. Dobbs, J. M. Wong, R. J. Lahiere, and K. P. Johnston, *Ind. Eng. Chem. Res.* **26**:56 (1987).
14. M. P. Ekart, K. L. Bennett, S. M. Ekart, G. S. Gurdial, C. L. Liotta, and C. A. Eckert, *AIChE J.* **39**:235 (1993).
15. K. M. Dooley, C.-P. Kao, R. P. Gambrell, and F. C. Knopf, *Ind. Eng. Chem. Res.* **26**:2058 (1987).
16. J. M. Dobbs and K. P. Johnston, *Ind. Eng. Chem. Res.* **26**:1476 (1987).
17. J. M. Dobbs, J. M. Wong, and K. P. Johnston, *J. Chem. Eng. Data* **31**:303 (1986).
18. W. J. Schmitt and R. C. Reid, *Fluid Phase Equilib.* **32**:77 (1986).

19. T. Vlachou, I. Prinos, J. Vera, and C. G. Panayiotou, *Ind. Eng. Chem. Res.* **41**:1057 (2002).
20. I. G. Economou and M. D. Donohue, *AIChE J.* **37**:1875 (1991).
21. W. G. Chapman, K. E. Gubbins, G. Jackson, and M. Radosz, *Ind. Eng. Chem. Res.* **29**:1709 (1990).
22. K. M. de Reuck and R. J. B. Craven, *International Thermodynamic Tables of the Fluid State – 12: Methanol* (Blackwell Scientific Publications, London, 1993).
23. R. D. Goodwin, *J. Phys. Chem. Ref. Data* **16**:799 (1987).
24. A. Polt, B. Platzter, and G. Maurer, *Chem. Tech. (Leipzig)* **44**:216 (1992).
25. J. R. S. Machado and W. B. Streett, *J. Chem. Eng. Data* **28**:218 (1983).
26. H. E. Dillon and S. G. Penoncello, *Int. J. Thermophys.* **25**:321 (2004).
27. A. D. Kozlov, *Methanol: Equations for Calculation of Thermophysical Properties* (Russian Research Center for Standardization, Information and Certification of Materials, Technical Report, Moscow, 2002).
28. P. T. Eubank, *Chem. Eng. Symp. Ser.* **66**:16 (1970).
29. M. M. Aliev, J. W. Magee, and I. M. Abdulagatov, *Int. J. Thermophys.* **24**:1527 (2003).
30. V. N. Zubarev, P. G. Prusakov, and L. V. Sergeev, *Thermophysical Properties of Methyl Alcohol* (GSSSD, Moscow, 1973).
31. V. N. Zubarev and A. V. Bagdonas, *Teploenergetika (Russ.)* **4**:79 (1967).
32. R. S. Finkelstein and L. I. Stiel, *Chem. Eng. Prog. Symp. Ser.* **66**:11 (1970).
33. W. Ramsay and S. Young, *Phil. Trans. R. Soc. London, Ser. A* **178**:313 (1887).
34. D. Ambrose and J. Walton, *Pure & Appl. Chem.* **61**:1396 (1989).
35. W. Wagner, *Cryogenics* **13**:470 (1973).
36. W. E. Donham, *VLE Data for 1-Methanol*, (Ph. D. Thesis Chemical Engineering Department, Ohio State University, 1953).
37. A. L. Lydersen and V. Tsochev, *Chem. Eng. Technol.* **13**:125 (1990).
38. J. M. Skaates and W. B. Kay, *Chem. Eng. Sci.* **19**:431 (1964).
39. T. W. de Loos, W. Poot, and J. de Swaan Arons, *Fluid Phase Equilib.* **42**:209 (1988).
40. D. Ambrose, C. H. S. Sprake, and R. Townsend, *J. Chem. Thermodyn.* **7**:185 (1975).
41. W. B. Kay and W. E. Donham, *Chem. Eng. Sci.* **4**:1 (1955).
42. Y. M. Suleimanov, *Ph. D. Thesis* (Thermophysics Department, Power Eng. Research Inst., Baku, 1971).
43. N. G. Polikhronidi, R. G. Batyrova, I. M. Abdulagatov, J. W. Magee, and G. V. Stepanov, *J. Supercritical Fluids* **33**:209 (2004).
44. I. Cibulka, *Fluid Phase Equilib.* **89**:1 (1993).
45. Y. V. Efremov, *Russ. J. Phys. Chem.* **40**:667 (1966).
46. H. Kitajima, N. Kagawa, H. Endo, S. Tsuruno, and J. W. Magee, *J. Chem. Eng. Data* **48**:1583 (2003).
47. T. Kuroki, N. Kagawa, H. Endo, S. Tsuruno, and J. W. Magee, *J. Chem. Eng. Data* **46**:1101 (2001).
48. S. Boyette and C. M. Criss, *J. Chem. Eng. Data* **33**:426 (1988).
49. M. M. Bashirov, *Isobaric Heat Capacity and Thermal Diffusivity of Alcohols and their Binary Mixtures* (ELM, Baku, 2003).
50. P. G. McCracken and J. M. Smith, *AIChE J.* **2**:498 (1956).
51. A. Lydersen, *Thesis* (IUPAC Center, 1986).
52. K. G. Akhmetzyanov, *Vestnik Moscovskogo Universiteta (Russ.)* **6**:93 (1949).
53. K. G. Akhmetzyanov, M. G. Shirkevich, and I. B. Rozhdestvenskii, *Primenenie Ul'trakust. Issledovaniy Veshestv (Russ.)* (MOPI, Moscow, 1957).
54. V. F. Nozdrev, *Acoustic J. (Russ.)* **2**:209 (1956).
55. J. B. Hannay, *Proc. Roy. Soc. London* **32**:294 (1882).

56. A. Nadejdine, *J. Russ. Phys. – Chem. Soc.* **14**:157 (1882).
57. P. de Heen, *Recheches Touchant la Physique Comparee et la Theories des Liquides* (Paris, 1888).
58. G. C. Schmidt, *Z. Phys. Chem.* **8**:628 (1891).
59. G. C. Schmidt, *Justus Liebigs Ann. Chem.* **266**:266 (1891).
60. M. Centnerszwer, *Z. Phys. Chem.* **49**:199 (1904).
61. L. Crismer, *Bull. Soc. Chim. Belg.* **18**:18 (1904).
62. E. Salwedel, *Ann. Phys. (Leipzig)* **5**:853 (1930).
63. A. Z. Golik, S. D. Ravikovich, and A. V. Orishchenko, *Ukr. J. Chem. (Russ.)* **21**:167 (1955).
64. R. F. Mocharnyuk, *Zh. Obshei Khimii (Russ.)* **30**:1098 (1960).
65. W. B. Kay, R. Khera, *Int. Data Ser., Selected Data Mixtures, Ser. A* **62**:1 (1975).
66. A. Z. Francesconi, H. Lentz, and E. U. Franck, *J. Phys. Chem.* **85**:3303 (1981).
67. E. Brunner, W. Hueltenschmidt, and G. Schlichthaerle, *J. Chem. Thermodyn.* **19**:273 (1987).
68. S. Young, *Sci. Proc. R. Dublin Soc* **12**:374 (1910).
69. R. Fischer and T. Reichel, *Mikrochem. Acta* **31**:102 (1943).
70. I. R. Krichevskii, N. E. Khazanova, and L. R. Lifshits, *Russ. J. Phys. Chem.* **31**:2711 (1957).
71. W. L. Marshall and E. V. Jones, *J. Inorg. Nucl. Chem.* **36**:2319 (1974).
72. N. G. Polikhronidi, I. M. Abdulagatov, and R. G. Batyrova, *Fluid Phase Equilib.* **201**:269 (2002).
73. D. Ambrose and C. L. Young, *J. Chem. Eng. Data* **40**:345 (1995).
74. L. C. Wilson, W. V. Wilding, H. L. Wilson, and G. M. Wilson, *J. Chem. Eng. Data* **40**:765 (1995).
75. D. J. Rosental and A. S. Teja, *AIChE J.* **35**:1829 (1989).
76. D. J. Rosental, M. T. Gude, A. S. Teja, and J. Mendez-Santiago, *Fluid Phase Equilib.* **135**:89 (1997).
77. E. D. Nikitin, P. A. Pavlov, and A. P. Popov, *Fluid Phase Equilib.* **149**:223 (1998).
78. D. M. Von Niederhausern, G. M. Wilson, and N. F. Giles, *J. Chem. Eng. Data* **45**:157 (2000).
79. E. D. Nikitin, P. A. Pavlov, and V. P. Skripov, *J. Chem. Thermodyn.* **25**:869 (1993).
80. M. Gude and A. S. Teja, *J. Chem. Eng. Data* **40**:1025 (1995).
81. N. G. Polikhronidi, R. G. Batyrova, and I. M. Abdulagatov, *Fluid Phase Equilib.* **175**:153 (2000).
82. N. G. Polikhronidi, I. M. Abdulagatov, J. W. Magee, and G. V. Stepanov, *Int. J. Thermophys.* **23**:745 (2002).
83. I. K. Kamilov, G. V. Stepanov, I. M. Abdulagatov, A. R. Rasulov, and E. I. Milikhina, *J. Chem. Eng. Data* **46**:1556 (2001).
84. I. M. Abdulagatov, N. G. Polikhronidi, and R. G. Batyrova, *J. Chem. Thermodyn.* **26**:1031 (1994).
85. I. M. Abdulagatov, N. G. Polikhronidi, and R. G. Batyrova, *Ber. Bunsenges. Phys. Chem.* **98**:1068 (1994).
86. N. G. Polikhronidi, I. M. Abdulagatov, J. W. Magee, and R. G. Batyrova, *J. Chem. Eng. Data* **46**:1064 (2001).
87. N. G. Polikhronidi, I. M. Abdulagatov, J. W. Magee, and G. V. Stepanov, *Int. J. Thermophys.* **22**:189 (2001).
88. N. G. Polikhronidi, R. G. Batyrova, and I. M. Abdulagatov, *Int. J. Thermophys.* **21**:1073 (2000).

89. N. G. Polikhronidi, I. M. Abdulagatov, J. W. Magee, and G. V. Stepanov, *Int. J. Thermophys.* **24**:405 (2003).
90. W. Wagner and A. Pruss, *J. Phys. Chem. Ref. Data* **31**:387 (2002).
91. N. B. Vargaftik, *Handbook of Physical Properties of Liquids and Gases* (Hemisphere Publishing Co., Washington, 1983).
92. L. Vlcek and I. Nezbeda, *Mol. Phys.* **102**:771 (2004).
93. A. K. Soper, F. Bruni, and M. A. Ricci, *J. Chem. Phys.* **106**:247 (1997).
94. M. M. Hoffman and M. S. Conradi, *J. Am. Chem. Soc.* **119**:3811 (1997).
95. J. L. Fulton, D. M. Pfund, S. L. Wallen, M. Newville, E. A. Stern, and Y. Ma, *J. Chem. Phys.* **105**:2161 (1996).
96. H. D. Eichholz, S. Schulz, and M. Wolf, *Kalte und Klimatechnik* **9**:322 (1981).
97. W. G. Chapman, K. E. Gubbins, G. Jackson, and M. Radosz, *Fluid Phase Equilib.* **52**:31 (1989).
98. H. Adidharma and M. Radosz, *Fluid Phase Equilib.* **161**:1 (1999).
99. M. Banaszak, Y. C. Chiew, and M. Radosz, *Phys. Rev. E:Stat. Phys., Plasmas, Fluids, Relat. Interdiscip. Top.* **48**:3760 (1993).
100. M. A. Anisimov and S. B. Kiselev, in *Sov. Tech. Rev. B. Therm. Phys., Part 2, Vol. 3, A. E. Scheindlin and V. E. Fortov, eds.* (Harwood Academic, New York, 1992), p. 1.
101. J. V. Sengers and J. M. H. Levelt Sengers, *Ann. Rev. Phys. Chem.* **37**:189 (1986).
102. M. A. Anisimov, S. B. Kiselev, J. V. Sengers, and S. Tang, *Physica A* **188**:487 (1992).
103. A. A. Povodyrev, G. X. Jin, S. B. Kiselev, and J. V. Sengers, *Int. J. Thermophys.* **17**:909 (1996).
104. M. Y. Belyakov, S. B. Kiselev, and J. C. Rainwater, *J. Chem. Phys.* **107**:3085 (1997).
105. K. S. Abdulkadirova, A. K. Wyczalkovaka, M. A. Anisimov, and J. V. Sengers, *J. Chem. Phys.* **116**:4597 (2002).
106. S. B. Kiselev, J. F. Ely, I. M. Abdulagatov, and M. L. Huber, *Ind. Eng. Chem. Res.* **44**:6916 (2005).
107. S. B. Kiselev, J. F. Ely, I. M. Abdulagatov, and J. W. Magee, *Int. J. Thermophys.* **21**:1373 (2000).
108. S. B. Kiselev and J. F. Ely, *Fluid Phase Equilib.* **222/223**:149 (2004).
109. L. Sun, S. B. Kiselev, and J. F. Ely, *Fluid Phase Equilib.* **233**:270 (2005).
110. S. B. Kiselev, *Fluid Phase Equilib.* **128**:1 (1997).
111. S. B. Kiselev and J. C. Rainwater, *J. Chem. Phys.* **109**:643 (1998).
112. S. B. Kiselev and J. C. Rainwater, *Fluid Phase Equilib.* **141**:129 (1997).
113. S. B. Kiselev, J. F. Ely, I. M. Abdulagatov, A. R. Bazaev, and J. W. Magee, *Ind. Eng. Chem. Res.* **41**:1000 (2002).
114. I. M. Abdulagatov, A. R. Bazaev, J. W. Magee, S. B. Kiselev, and J. F. Ely, *Ind. Eng. Chem. Res.* **44**:1967 (2005).
115. L. D. Landau and E. M. Lifshitz, *Statistical Physics, Part 1* (Pergamon Press, New York, 1980).
116. A. Z. Patashinskii and V. L. Pokrovskii, *Fluctuation Theory of Phase Transitions* (Pergamon Press, New York, NY, 1979).
117. S. B. Kiselev, *High. Temp.* **28**:47 (1990).
118. M. Y. Belyakov and S. B. Kiselev, *Physica A* **190**:75 (1992).
119. P. G. McCracken, T. S. Storvick, and J. M. Smith, *J. Chem. Eng. Data* **5**:130 (1960).
120. J. M. Costello and S. T. Bowden, *Rec. Trav. Chim. Pays-Bas.* **77**:36 (1958).
121. D. Ambrose, *Correlation and Estimation of Vapour-Liquid Critical Properties I. Critical Temperatures of Organic Compounds, Report Chem 92*, National Physical Laboratory Teddington, United Kingdom (1978).
122. S. M. Loktev, *High Fat Alcohols* (Khimiya, Moscow, 1970).

123. R. H. Harrison and B. E. Gammon, private communication to IUPAC Centre (1989); Table in K. M. de Reuck and R. J. B. Craven, *International Thermodynamic Tables of the Fluid State - 12: Methanol* (Blackwell Scientific Publications, London, 1993), p. 83.
124. J. M. Simonson, D. J. Bradley, and R. H. Busey, *J. Chem. Thermodyn.* **19**:479 (1987).
125. K. A. Kobe and R. E. Lynn, Jr., *Chem. Rev.* **52**:117 (1953).
126. A. P. Kudchadker, G. H. Alani, and B. J. Zwolinski, *Chem. Rev.* **68**:659 (1968).
127. R. C. Wilhoit and B. J. Zwolinski, *J. Phys. Chem. Ref. Data (Suppl.)* **2**:423 pp (1973).
128. J. M. Smith and R. Srivastava, *Phys. Sciences Data* (Elsevier, Amsterdam, 1986).
129. R. J. B. Craven and K. M. de Reuck, *Int. J. Thermophys.* **7**:541 (1986).
130. D. Ambrose and C. H. S. Sprake, *J. Chem. Thermodyn.* **2**:631 (1970).
131. O. Osada, M. Sato, and M. Uematsu, *J. Chem. Thermodyn.* **31**:451 (1999).
132. V. Niesen, A. M. F. Palavra, A. J. Kidney, and V. F. Yesavage, *Fluid Phase Equilib.* **31**:283 (1986).
133. R. A. Wilsak, S. W. Campell, and G. Thodos, *Fluid Phase Equilib.* **28**:13 (1985).
134. M. Hirata and S. Suda, *Kagaku Kogaku* **31**:339 (1967).
135. J. L. Hales and J. H. Ellender, *J. Chem. Thermodyn.* **8**:1177 (1976).
136. F. Vesely, L. Svab, R. Provaznik, and V. Svoboda, *J. Chem. Thermodyn.* **20**:981 (1988).
137. M. Radosz and A. Lydersen, *Chem.-Ing.-Tech.* **52**:756 (1980).